Euro. Jnl of Applied Mathematics (2013), *vol.* 24, *pp.* 803–833. © Cambridge University Press 2013 803
doi:10.1017/S095679251300020X

Formal derivation of a bilayer model coupling shallow water and Reynolds lubrication equations: evolution of a thin pollutant layer over water

E. D. FERNÁNDEZ-NIETO[1], G. NARBONA-REINA[1] and J. D. ZABSONRÉ[2]

[1]*Departamento Matemática Aplicada I, Universidad de Sevilla, Seville, Spain*
emails: edofer@us.es, gnarbona@us.es
[2]*Unité de Formation et de Recherche en Sciences et Techniques, Département de Mathématiques, Université Polytechnique de Bobo-Dioulasso, Bobo-Dioulasso, Burkina Faso*
email: jzabsonre@gmail.com

(*Received 25 January 2012; revised 29 May 2013; accepted 30 May 2013; first published online 27 June 2013*)

In this paper, a bilayer model is derived to simulate the evolution of a thin film flow over water. This model is derived from the incompressible Navier–Stokes equations together with suitable boundary conditions including friction and capillary effects. The derivation is based on the different properties of the fluids; thus, we perform a multiscale analysis in space and time, and a different asymptotic analysis to derive a system coupling two different models: the Reynolds lubrication equation for the upper layer and the shallow water model for the lower one. We prove that the model verifies a dissipative entropy inequality up to a second-order term. Moreover, we propose a correction of the model – by taking into account the second-order extension for the pressure – that admits an exact dissipative entropy inequality. Two numerical tests are presented. In the first test, we compare the numerical results with the viscous bilayer shallow water model proposed in Narbona-Reina *et al.* (*Comput. Model. Eng. Sci.,* 2009, Vol. 43, pp. 27–71). In the second test, the objective is to show some of the characteristic situations that can be studied with the proposed model. We simulate a problem of pollutant dispersion near the coast. For this test, the influence of the friction coefficient on the coastal area affected by the pollutant is studied.

Key words: Bilayer model, Reynolds equation, shallow water, multiscale analysis

1 Introduction

In this paper, we derive a bilayer model of two immiscible fluids where the upper layer can be represented by a Reynolds lubrication model and the lower layer by a shallow water model. This model can be used to simulate the evolution of a pollutant viscous fluid over water.

Our purpose is to study the evolution of a system that consists of two layers of Newtonian viscous fluids with different properties. For the upper layer, we consider a thin liquid film of slow flow – Reynolds number of unity order – and for the lower one, we assume a fluid-like water – high Reynolds number. Under these assumptions, it is not possible to choose the same type of equations to model each layer.

Thus, for the upper layer, we follow the Reynolds' theory of lubrication to deduce the equation that defines its behaviour. In this equation, the pressure plays the main role. The Reynolds lubrication equation is classically used to model a fluid between two very close surfaces or a very thin film. This equation was first derived in [24], where several hypotheses are used in order to describe the pressure of the film. In fact, in this derivation, inertial, gravitational, viscosity variation, slip condition at the bottom, surface roughness and thermal effects are neglected. In addition, the author restricts his analysis to an isoviscous, incompressible fluid. Later, much research related to the derivation of the generalized Reynolds lubrication equation has been made in order to get a better modelling of a thin film (see for example [7, 8, 11, 12, 19, 28, 30]).

In [21], a review of the long-scale evolution of thin liquid films is presented. A general mathematical theory of Reynolds lubrication equations is introduced. In their analysis, the authors use the slip condition at the bottom and take into account surface tension effects at the free surface. A general nonlinear evolution equation or equations are then derived and several particular cases are considered. The condition on the free surface with surface tension effects revealed the presence of a term of the form $\partial_x(\sigma\partial_x^2 h)$, where σ is the surface tension coefficient and h is the height of the thin layer. This term appears at the leading order due to the scaling used for this purpose.

In another way, the shallow water system, which is considered to model the lower layer, is applied to study a large number of geophysical and engineering applications such as ocean circulation, coastal areas, rivers, etc. Many derivations of this model had been made in order to model shallow flows (see for example [1, 4, 13, 20, 23, 33]). The pioneering work [14] has been considered as a basis to develop the deduction of the shallow water layer of the model proposed in this paper. This derivation takes into account laminar friction at the bottom and viscous effects. Viscous and capillary effects are useful to obtain an existence result of global weak solutions in [34]. In [18], a viscous two-dimensional one-layer shallow water system, taking into account surface tension, capillary effects and quadratic friction terms, has been derived. In [20], the authors derived a bilayer shallow water model where friction and surface tension at the interface and free surface are introduced with a second-order approximation.

In the model considered in this work, coupling Reynolds lubrication and shallow water equations, the shallow-flow assumption is taken, that is, the height (H) of the layer is much smaller than its length (L). Thus, for the derivation of the model, all the variables are written in terms of this aspect ratio $\varepsilon = H/L$, assumed small. As mentioned above, the obtention of the model is inspired from the simulation of the transport of a pollutant over water. Therefore, following this idea, we consider that this smallness ratio ε is not the same for the two layers. This means that the order of all the characteristic variables, namely, velocities, pressures, viscosities, space and time, is different for each layer. Due to these hypotheses, the idea of the present work is to make a multiscale analysis in space and time for the incompressible bilayer Navier–Stokes equations and obtain a simplified system of three equations.

In the literature, one can find several papers related to the multiscale analysis in time in order to model the evolution of the topography in oceans submitted to tidal effects, see for example [9, 15, 25, 27].

The novelty of this work rests on two features, which, to the best of our knowledge, have not been tackled before in the modelling of multilayer systems. The first is the coupling of two different equations on a bilayer model and the second is the multiscale analysis – in space and time – developed in the two layers. Both also provide the main difficulties in deriving the proposed model.

This paper is organized as follows. Section 2 is devoted to the derivation of the model. First, we write the equations in non-dimensional variables, taking into account a different scale for each layer. Next, to deduce the shallow water equation, we first perform the hydrostatic approximation and use an asymptotic analysis to deduce the shallow water system. We also use an asymptotic analysis to deduce a Reynolds lubrication equation for the upper layer. In Section 3, we present the obtained model and in Section 3.1 we study the energy of the model. Finally, in Section 4, we describe a numerical scheme to discretize the proposed model and two numerical tests.

2 The thin film – shallow water model

In this section, we give a formal derivation of the model. To deduce the model, we start from the incompressible Navier–Stokes equations for both layers and follow the following steps: first, we non-dimensionalize equations, then we take into account the asymptotic regime for the physical parameters and finally we integrate the equations to get the averaged model.

Following the goal of this work, we search for a bilayer model where each one of the fluids has different properties. Therefore, we consider that they have not only different physical properties but also a different flow behaviour.

As mentioned before, we use this model to simulate the evolution of a pollutant over water, so we also consider different thickness for each layer.

All these considerations imply some difficulties to develop the derivation of the model. First, due to the different flow behaviour, we must follow different ways to obtain the equations that model each layer. For the lower layer, we derive a shallow water model and a Reynolds lubrication equation is used for the upper layer. The fact of considering different thicknesses leads us to take different characteristic space variables. Moreover, in order to take into account the ‘slow flow’ property for the fluid on the upper layer we also consider different characteristic velocities. Thus, we must develop a two-scale analysis of the problem in space and time.

First, we introduce the domain of study and set out the incompressible Navier–Stokes equations together with appropriate boundary conditions. In particular, the interaction between the two fluids is held in the interface boundary conditions through the friction and capillary effects. We also take into account capillary effects at the free surface and friction force at the bottom.

We consider the two-dimensional domain $\Omega(t) = \Omega_1(t) \cup \Omega_2(t) \cup \Gamma_b \cup \Gamma_{1,2}(t) \cup \Gamma_s(t)$, where

$$\begin{aligned}
\Omega_1(t) &= \{(x,z) \in \mathbb{R}^2 : x \in \omega,\ b(x) < z < \mathscr{I}(x,t)\},\\
\Omega_2(t) &= \{(x,z) \in \mathbb{R}^2 : x \in \omega,\ \mathscr{I}(x,t) < z < \eta(x,t)\},\\
\Gamma_{1,2}(t) &= \{(x,z) \in \mathbb{R}^2 : x \in \omega,\ z = \mathscr{I}(x,t)\},\\
\Gamma_s(t) &= \{(x,z) \in \mathbb{R}^2 : x \in \omega,\ z = \eta(x,t)\},\\
\Gamma_b &= \{(x,z) \in \mathbb{R}^2 : x \in \omega,\ z = b(x)\},
\end{aligned}$$

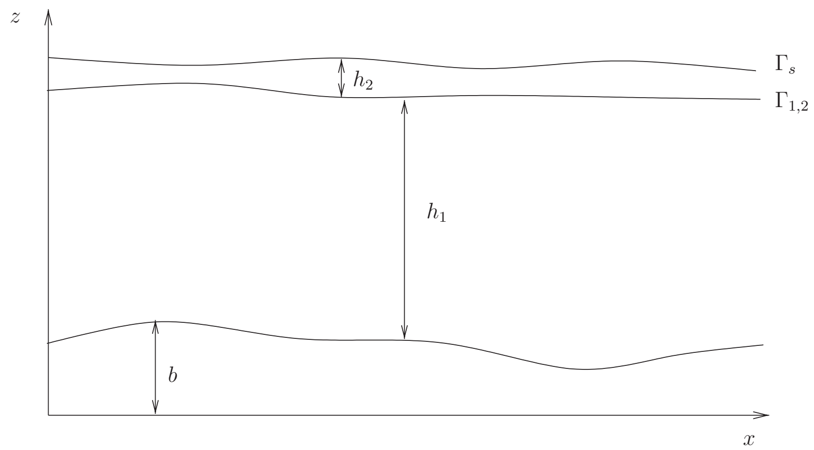

FIGURE 1. Schematic representation of the two layers over the solid boundary b, with the free surface denoted by Γ_s, the interface between the two fluids, $\Gamma_{1,2}$, and heights labelled h_1 and h_2.

and ω is a bounded domain in $\mathbb{R}$. We denote by $\mathscr{I}$ the interface level, $\mathscr{I}(x,t) = b(x) + h_1(x,t)$, and by η the free surface, $\eta(x,t) = b(x) + h_1(x,t) + h_2(x,t)$ (see Figure 1).

We consider the incompressible Navier–Stokes equations for each layer:

$$\begin{cases} \rho_i(\partial_t u_i + u_i\partial_x u_i + w_i\partial_z u_i) = -\partial_x p_i + \rho_i \nu_i(\partial_x^2 u_i + \partial_z^2 u_i), \\ \rho_i(\partial_t w_i + u_i\partial_x w_i + w_i\partial_z w_i) = -\partial_z p_i + \rho_i \nu_i(\partial_x^2 w_i + \partial_z^2 w_i) - \rho_i g, \\ \partial_x u_i + \partial_z w_i = 0, \end{cases} \qquad i = 1,2. \tag{2.1}$$

where we denote by $v_i = (u_i, w_i)$ the velocity field for each layer, ρ_i the density, ν_i is the kinematic viscosity and p_i the pressure, for $i = 1,2$; g is the constant gravity. As a general notation rule, the subscript 1 corresponds to the lower layer and the subscript 2 to the upper layer. We also introduce the ratio of densities

$$r = \frac{\rho_2}{\rho_1}$$

and the stress tensors $\sigma_i = 2\rho_i\nu_i D(v_i) - p_i \mathrm{Id}$, where $D(v_i) = \frac{\nabla v_i + \nabla v_i^T}{2}$ and Id denotes the identity matrix.

To complete the problem, we impose the following boundary conditions:

- At the free surface, $z = \eta(x,t)$:
  - The normal stress balance:

$$(\sigma_2 \cdot n_s) = -\delta\, \kappa n_s, \tag{2.2}$$

    where δ is the surface tension coefficient, $\kappa = -\mathrm{div}_x n_s$ is the mean curvature and n_s the unitary outward normal vector to the free surface, $n_s = \frac{1}{\sqrt{1+|\partial_x \eta|^2}}(-\partial_x \eta,\ 1)$.
  - The kinematic condition:

$$\partial_t \eta + u_2\, \partial_x \eta = w_2. \tag{2.3}$$

https://doi.org/10.1017/S095679251300020X Published online by Cambridge University Press

- At the interface, $z = \mathscr{I}(x,t)$:
  - The kinematic conditions for each velocity:

$$\begin{aligned} \partial_t h_1 + u_2\,\partial_x \mathscr{I} &= w_2, \\ \partial_t h_1 + u_1\,\partial_x \mathscr{I} &= w_1. \end{aligned} \tag{2.4}$$

  - The normal stress balance:

$$(\sigma_1 \cdot n_{\mathscr{I}})_n - (\sigma_2 \cdot n_{\mathscr{I}})_n = (\delta_{\mathscr{I}}\, \kappa_{\mathscr{I}} n_{\mathscr{I}})_n, \tag{2.5}$$

    with $\delta_{\mathscr{I}}$ the interfacial tension coefficient, $\kappa_{\mathscr{I}} = -\mathrm{div}_x n_{\mathscr{I}}$ is the mean curvature of the interface and $n_{\mathscr{I}} = \frac{1}{\sqrt{1+|\partial_x \mathscr{I}|^2}}(-\partial_x \mathscr{I},\ 1)$, the unitary normal vector to the interface pointing from layer 1 to layer 2. The subscript n denotes the normal component of the vector.
  - The friction condition (Navier-slip boundary condition):

$$(\sigma_i \cdot n_{\mathscr{I}})_\tau = -c\rho_2(v_1 - v_2)_\tau \quad \text{for } i = 1, 2. \tag{2.6}$$

    The positive friction coefficient is denoted by c. The subscript τ denotes the tangential component of the vector.

- At the bottom, $z = b(x)$:
  We consider the Navier-slip boundary conditions:
  - The no-penetration condition:

$$v_1 \cdot n_b = 0, \tag{2.7}$$

    where $n_b = \frac{1}{\sqrt{1+|\partial_x b|^2}}(-\partial_x b,\ 1)$.
  - The friction condition:

$$(\sigma_1 \cdot n_b)_\tau = \alpha(u_1)_\tau, \tag{2.8}$$

    where α is the positive friction coefficient.

Remark 2.1 A linear friction term between the two layers is considered here. It coincides with the friction law used in [20] that is of the form $c(v_1 - v_2)$. In [6], this type of a friction term is used to study a system of 3D Navier–Stokes equations in a two-layer thin domain with an interface condition of the form $(v_i \partial_z u_j^i - k(u_j^1 - u_j^2)) = 0,\ i, j = 1, 2$.

2.1 Dimensionless equations

To derive the model, it is suitable to write the system (2.1)–(2.8) in dimensionless form. First, let us divide the conservation equations by densities ρ_i to get

$$\begin{cases} \partial_t u_i + u_i \partial_x u_i + w_i \partial_z u_i &= -\frac{1}{\rho_i}\partial_x p_i + v_i(\partial_x^2 u_i + \partial_z^2 u_i), \\ \partial_t w_i + u_i \partial_x w_i + w_i \partial_z w_i &= -\frac{1}{\rho_i}\partial_z p_i + v_i(\partial_x^2 w_i + \partial_z^2 w_i) - g, \\ \partial_x u_i + \partial_z w_i = 0. \end{cases} \tag{2.9}$$

https://doi.org/10.1017/S095679251300020X Published online by Cambridge University Press

Now we set the dimensionless variables, where we must take into account the different properties of the fluids in two layers, so we make it separately. Nevertheless, the characteristic variables of both layers must be related because we study the coupled system. We must indicate that the Reynolds layer is not only thin and slow, but thinner and slower than the shallow water layer. Thus, we will make an assumption relating the aspect ratios of the two layers.

Non-dimensionalization for layer 1

First, we establish the dimensionless variables for the lower layer following a shallow water non-dimensionalization (see [14]). We denote by H, L and U the characteristic height, length and velocity, respectively. Thus, the characteristic time is $T = L/U$. To impose the shallow flow condition, we assume that the aspect ratio between the characteristic height and length is small, as commonly we denote it by $\varepsilon = H/L$. We denote with the superscript asterisk (*) the dimensionless variables:

$$\begin{aligned} x &= Lx^*, & z_1 &= Hz_1^*, & h_1 &= Hh_1^*, \\ u_1 &= Uu_1^*, & w_1 &= \varepsilon U w_1^*, & t &= Tt_1^*, \\ p_1 &= \rho_1 U^2 p_1^*, & Fr_1 &= \frac{U}{\sqrt{gH}}, & Re_1 &= \frac{UL}{\nu_1}, \end{aligned}$$

where we denoted by Fr_1 the Froude number and by Re_1 the Reynolds number.

Non-dimensionalization for layer 2

For the upper layer, we take a non-dimensionalization suitable for a Reynolds lubrication equation following [21]. It mainly affects the characteristic pressure, which is larger due to the lubrication effect. Now we denote by H_2, U_2 and $T_2 = L/U_2$ the characteristic height, velocity and time for this layer, respectively. Thus, we also have a different ratio height–length, namely, $\varepsilon_2 = H_2/L$. The dimensionless variables in this case are

$$\begin{aligned} x &= Lx^*, & z_2 &= H_2 z_2^*, & h_2 &= H_2 h_2^*, \\ u_2 &= U_2 u_2^*, & w_2 &= \varepsilon_2 U_2 w_2^*, & t &= T_2 t_2^*, \\ p_2 &= \frac{\rho_2 \nu_2 U_2}{\varepsilon_2 H_2} p_2^*, & Fr_2 &= \frac{U_2}{\sqrt{gH_2}}, & Re_2 &= \frac{U_2 L}{\nu_2}. \end{aligned}$$

Since we study the coupled system, we must take into account that layer 2 is thinner and slower than layer 1. These related aspects lead us to search for a relationship between the characteristic height and velocity of the two layers that express these properties. Thus, we assume that

$$H_2 = \varepsilon H, \qquad U_2 = \varepsilon^2 U,$$

consequently, $\varepsilon_2 = \varepsilon^2$ and $T_2 = \frac{1}{\varepsilon^2} T$.

https://doi.org/10.1017/S095679251300020X Published online by Cambridge University Press

We write the dimensionless variables of layer 2 in terms of H, U and ε:

$$x = Lx^*, \qquad z_2 = \varepsilon H z_2^*, \qquad h_2 = \varepsilon H h_2^*,$$
$$u_2 = \varepsilon^2 U u_2^*, \qquad w_2 = \varepsilon^4 U w_2^*, \qquad t = \frac{1}{\varepsilon^2} T t_2^*,$$
$$p_2 = \frac{\rho_2 \nu_2 U}{\varepsilon H} p_2^*, \qquad Fr_2 = \frac{\varepsilon^2 U}{\sqrt{g\varepsilon H}}, \qquad Re_2 = \frac{\varepsilon U H}{\nu_2}.$$

Remark 2.2 We give some remarks about the dimensionless procedure. First, to justify our hypothesis on the aspect ratio $\varepsilon_2 = \varepsilon^2$, we focus on the oceanic circulation case. In accordance with [18], the average thickness H of the oceans in the coastal domain is nearly 100 m, whereas their horizontal characteristic value is about 100 km. So, the aspect ratio $\varepsilon = H/L$ is about 10^{-3}. Thus, we are in the case that the pollutant layer has an aspect ratio of $\epsilon_2 \sim 10^{-6}$ and a thickness 10^{-3} times smaller than layer 1, which is equivalent to a thickness of $H_2 = \varepsilon H \sim 10cm$, which seems reasonable. Second, we clarify the existence of two dimensionless times t_1^* and t_2^*. It just comes from considering two characteristic velocities which automatically give two different characteristic times T and $T_2 = \frac{1}{\varepsilon^2} T$. Therefore, the times do not have the same order, that is why we also consider two dimensionless times.

Regarding the friction coefficients, we take

$$\alpha = U\alpha^*, \quad c = Uc^*,$$

and the Capillary numbers – at the free surface (C) and the interface ($C_{\mathscr{I}}$) – as

$$C = \frac{\varepsilon^2 U \rho_2 \nu_2}{\delta}, \quad C_{\mathscr{I}} = \frac{U \rho_1 \nu_1}{\delta_{\mathscr{I}}}.$$

We assume H as the characteristic height for the bottom, so $b = Hb^*$.

Due to the different characteristic heights, we must pay attention to the ranges for the dimensionless vertical component. Thus, for layer 1, since $z_1 \in [b, b + h_1]$, we obtain directly that $z_1^* \in [b^*, b^* + h_1^*]$. For layer 2, the rank of the dimensional variable is $z_2 \in [b + h_1, b + h_1 + h_2]$, so we deduce that $z_2^* \in [\frac{1}{\varepsilon}(b^* + h_1^*), \frac{1}{\varepsilon}(b^* + h_1^*) + h_2^*]$. In what follows – for the second layer – we denote $\eta_\varepsilon = \frac{1}{\varepsilon}(b^* + h_1^*) + h_2^*$ as the free surface level and $\mathscr{I}_\varepsilon = \frac{1}{\varepsilon}(b^* + h_1^*)$ the interface level. Next, we write the equations and the boundary conditions in dimensionless form, and omit the superscript (*) in the notation for the sake of clarity.

• *Layer 1*

$$\partial_{t_1} u_1 + u_1 \partial_x u_1 + w_1 \partial_z u_1 - \frac{1}{Re_1}\left(\partial_x^2 u_1 + \frac{1}{\varepsilon^2}\partial_z^2 u_1\right) + \partial_x p_1 = 0, \tag{2.10}$$

$$\partial_{t_1} w_1 + u_1 \partial_x w_1 + w_1 \partial_z w_1 - \frac{1}{Re_1}\left(\partial_x^2 w_1 + \frac{1}{\varepsilon^2}\partial_z^2 w_1\right) + \frac{1}{\varepsilon^2}\partial_z p_1 = -\frac{1}{\varepsilon^2}\frac{1}{Fr_1^2}, \tag{2.11}$$

$$\partial_x u_1 + \partial_z w_1 = 0. \tag{2.12}$$

https://doi.org/10.1017/S095679251300020X Published online by Cambridge University Press

- *Layer 2*

$$
\begin{aligned}
\varepsilon^4 Re_2(\partial_{t_2}u_2 + u_2\partial_x u_2 + w_2\partial_{z_2}u_2) &= -\partial_x p_2 + \partial^2_{z_2}u_2 + \varepsilon^4\partial^2_x u_2,\\
\varepsilon^8 Re_2(\partial_{t_2}w_2 + u_2\partial_x w_2 + w_2\partial_{z_2}w_2) &= -\partial_{z_2}p_2 - \varepsilon^4\tfrac{Re_2}{Fr_2^2} + \varepsilon^4(\partial^2_{z_2}w_2 + \varepsilon^4\partial^2_x w_2),\\
\partial_x u_2 + \partial_{z_2}w_2 &= 0.
\end{aligned}
\tag{2.13}
$$

- *Conditions at the free surface*

$$
\partial_{t_1}(b+h_1) + \varepsilon^3\partial_{t_2}h_2 + \varepsilon^2 u_2\,\partial_x(b+h_1) + \varepsilon^3 u_2\partial_x h_2 = \varepsilon^3 w_2,
\tag{2.14}
$$

$$
(\partial_{z_2}u_2 + \varepsilon^4\partial_x w_2)(1-\varepsilon^2(\partial_x(b+h_1+\varepsilon h_2))^2) - 4\varepsilon^3\partial_x u_2\,\partial_x(b+h_1+\varepsilon h_2) = 0,
\tag{2.15a}
$$

$$
\begin{aligned}
&-p_2 + 2\varepsilon^4\partial_z w_2 - \varepsilon^3\partial_x(b+h_1+\varepsilon h_2)(\partial_{z_2}u_2 + \varepsilon^4\partial_x w_2)\\
&\quad = -\varepsilon^5\frac{C^{-1}\partial^2_x(b+h_1+\varepsilon h_2)}{(1+\varepsilon^2(\partial_x(b+h_1+\varepsilon h_2))^2)^{3/2}}.
\end{aligned}
\tag{2.15b}
$$

- *Conditions at the interface*

$$
\partial_{t_1}(b+h_1) + \varepsilon^2 u_2\,\partial_x(b+h_1) = \varepsilon^3 w_2,
\tag{2.16}
$$

$$
\partial_{t_1}(b+h_1) + u_1\,\partial_x(b+h_1) = w_1,
\tag{2.17}
$$

$$
\begin{aligned}
&-2\rho_1\frac{1}{Re_1}(\varepsilon^2\partial_x w_1 + \partial_z u_1)\partial_x(b+h_1) + \varepsilon^2\rho_1\left(2\frac{1}{Re_1}\partial_x u_1 - p_1\right)\partial_x(b+h_1)^2\\
&\quad + \rho_1\left(2\frac{1}{Re_1}\partial_z w_1 - p_1\right) = -2\rho_2\frac{1}{Re_2}\varepsilon^3\left(\varepsilon^4\partial_x w_2 + \partial_{z_2}u_2\right)\partial_x(b+h_1)\\
&\quad + \varepsilon^2\frac{1}{Re_2}\rho_2(2\varepsilon^4\partial_x u_2 - p_2)\partial_x(b+h_1)^2 + \rho_2\frac{1}{Re_2}(2\varepsilon^4\partial_z w_2 - p_2)\\
&\quad + \varepsilon\rho_1\frac{C_{\mathscr{I}}^{-1}}{Re_1}\partial^2_x(b+h_1)(1+\varepsilon^2\partial_x(b+h_1)^2),
\end{aligned}
\tag{2.18}
$$

$$
\begin{aligned}
&-4\frac{1}{Re_1}\partial_x u_1\partial_x(b+h_1) + \frac{1}{Re_1}(\partial_x w_1 + \frac{1}{\varepsilon^2}\partial_z u_1)(1-\varepsilon^2\partial_x(b+h_1)^2)\\
&\quad = -\frac{r}{\varepsilon}c(u_1 - \varepsilon^2 u_2 + \varepsilon^2(w_1 - \varepsilon^3 w_2)\partial_x(b+h_1)),
\end{aligned}
\tag{2.19}
$$

$$
\begin{aligned}
&-4\varepsilon^4\frac{1}{Re_2}\partial_x u_2\partial_x(b+h_1) + \varepsilon\frac{1}{Re_2}(\varepsilon^4\partial_x w_2 + \partial_{z_2}u_2)(1-\varepsilon^2\partial_x(b+h_1)^2)\\
&\quad = -\frac{1}{\varepsilon}c(u_1 - \varepsilon^2 u_2 + \varepsilon^2(w_1 - \varepsilon^3 w_2)\partial_x(b+h_1)).
\end{aligned}
\tag{2.20}
$$

https://doi.org/10.1017/S095679251300020X Published online by Cambridge University Press

- *Conditions at the bottom*

$$-u_1\,\partial_x b + w_1 = 0, \tag{2.21}$$

$$\begin{aligned} &-\rho_1\frac{4}{Re_1}\partial_x u_1\partial_x b + \rho_1\frac{1}{Re_1}\left(\partial_x w_1 + \frac{1}{\varepsilon^2}\partial_z u_1\right)\\ &-\varepsilon^2\rho_1\frac{1}{Re_1}\left(\partial_x w_1 + \frac{1}{\varepsilon^2}\partial_z u_1\right)(\partial_x b)^2 = \frac{\alpha}{\varepsilon}u_1(1+\varepsilon^2(\partial_x b)^2). \end{aligned} \tag{2.22}$$

In the next subsections, we develop the derivation of the equations for both layers. We begin with the shallow water layer following [14, 20] and then deduce the Reynolds lubrication layer following [21]. In order to get the viscous effect and the influence of the pressure of the thin film flow on the system, we derive a second-order approximation, that is, we keep the terms of order ε^0 and ε in the system.

2.2 Layer 1: shallow water flow

To obtain the shallow water model, we first take the hydrostatic approximation and then develop the asymptotic analysis of (2.10).

2.2.1 *Hydrostatic approximation*

To obtain the averaged model, we integrate each equation into $[b, b+h_1]$.
We first integrate (2.10) to get

$$\begin{aligned} &\partial_{t_1}\left(\int_b^{b+h_1} u_1 dz\right) + \partial_x\left(\int_b^{b+h_1} u_1^2 dz\right) + \int_b^{b+h_1}\partial_x p_1 dz - \frac{1}{Re_1}\partial_x\left(\int_b^{b+h_1}\partial_x u_1 dz\right)\\ &-u_{1|_{\mathscr{I}}}(\partial_{t_1}h_1 + u_1\partial_x(b+h_1) - w_1)_{|_{\mathscr{I}}} - u_{1|_b}w_{1|_b} + u_{1|_b}^2\,\partial_x b\\ &-\frac{1}{Re_1}\partial_x u_{1|_b}\partial_x b + \frac{1}{Re_1}\partial_x u_{1|_{\mathscr{I}}}\partial_x(b+h_1) - \frac{1}{\varepsilon^2}\frac{1}{Re_1}\partial_z u_{1|_{\mathscr{I}}} + \frac{1}{\varepsilon^2}\frac{1}{Re_1}\partial_z u_{1|_b} = 0. \end{aligned} \tag{2.23}$$

Now, we simplify this equation by using the conditions at the bottom and at the interface. In particular, we use equations (2.17), (2.19), (2.21) and (2.22) at order ε^2. Then we write (2.23) up to second order as

$$\begin{aligned} &\partial_{t_1}\left(\int_b^{b+h_1} u_1 dz\right) + \partial_x\left(\int_b^{b+h_1} u_1^2 dz\right) + \int_b^{b+h_1}\partial_x p_1 dz - \frac{1}{Re_1}\partial_x\left(\int_b^{b+h_1}\partial_x u_1 dz\right)\\ &+\frac{1}{Re_1}(\partial_x w_1 - 3\partial_x u_1\partial_x(b+h_1))_{|_{\mathscr{I}}} - \frac{1}{Re_1}(\partial_x w_1 - 3\partial_x u_1\partial_x b)_{|_b}\\ &+\frac{1}{\varepsilon}rc(u_{1|_{\mathscr{I}}} - \varepsilon^2 u_{2|_{\mathscr{I}_\varepsilon}} + \varepsilon^2 w_{1|_{\mathscr{I}}}\partial_x(b+h_1)) + \frac{1}{\rho_1\varepsilon}\alpha u_{1|_b} = 0. \end{aligned} \tag{2.24}$$

To find p_1, we use the equation of the vertical velocity. From equation (2.12), we can write

$$-\frac{1}{Re_1}\partial_z^2 w_1 + \partial_z p_1 = -\frac{1}{Fr_1^2} + \mathcal{O}(\varepsilon^2). \tag{2.25}$$

https://doi.org/10.1017/S095679251300020X Published online by Cambridge University Press

Now, we integrate this equation from z to $(b+h_1)$ and use the divergence-free condition (2.12) to get up to second order:

$$p_1(z) = p_{1|_{\mathscr{I}}} - \frac{1}{Re_1}(\partial_x u_1 - \partial_x u_{1|_{\mathscr{I}}}) - \frac{1}{Fr_1^2}(z-(b+h_1)). \tag{2.26}$$

2.2.2 *Asymptotic analysis*

We assume the following asymptotic regime for the data:

$$v_1 = \mathscr{O}(\varepsilon), \quad \alpha = \mathscr{O}(\varepsilon), \quad c = \mathscr{O}(\varepsilon), \quad \delta_{\mathscr{I}} = \mathscr{O}(\varepsilon^{-2}),$$

so for simplicity we write

$$\frac{1}{Re_1} = \varepsilon\mu_{01}, \quad \alpha = \varepsilon\alpha_0, \quad c = \varepsilon c_0, \quad C_{\mathscr{I}}^{-1} = \varepsilon^{-2}C_{\mathscr{I}0}^{-1}. \tag{2.27}$$

Since we look for a second-order approximation, we develop the unknowns at order 1 and define

$$\tilde{h}_1 = h_1^0 + \varepsilon h_1^1, \quad \tilde{u}_1 = u_1^0 + \varepsilon u_1^1, \quad \tilde{p}_1 = p_1^0 + \varepsilon p_1^1,$$

which are the unknowns of the problem for layer 1.

Taking into account (2.27), we write from (2.10), (2.19) and (2.22) that

$$\begin{aligned} \partial_z^2 u_1 &= \mathscr{O}(\varepsilon), \\ \partial_z u_{1|_{\mathscr{I}}} &= \mathscr{O}(\varepsilon), \\ \partial_z u_{1|_b} &= \mathscr{O}(\varepsilon). \end{aligned}$$

Then, u_1 does not depend on z at first order, so $u_1^0(x,z,t) = u_1^0(x,t)$. From (2.12), we can write the mass equation for h_1^0:

$$\partial_{t_1} h_1^0 + \partial_x(h_1^0 u_1^0) = 0. \tag{2.28}$$

To obtain the momentum equation, we first simplify (2.26). We get

$$p_1^0(z) = p_{1|_{\mathscr{I}}}^0 - \frac{1}{Fr^2}(z-(b+h_1^0)), \tag{2.29}$$

so $p_1^0(b) = p_{1|_{\mathscr{I}}}^0 + \dfrac{1}{Fr^2}h_1^0$. Thus, we calculate the integral appearing in (2.24),

$$\int_b^{b+h_1} \partial_x p_1^0 \, dz = h_1^0 \partial_x(p_{1|_{\mathscr{I}}}^0) + \frac{1}{Fr_1^2} h_1^0 \partial_x(b+h_1^0).$$

https://doi.org/10.1017/S095679251300020X Published online by Cambridge University Press

If we substitute this expression into (2.24) and consider only principal order terms, we obtain

$$\partial_{t_1}(h_1^0 u_1^0) + \partial_x(h_1^0 (u_1^0)^2) + h_1^0 \partial_x (p^0_{1_{|\mathscr{I}}}) + \frac{1}{2}\frac{1}{Fr_1^2}\partial_x (h_1^0)^2 + \frac{1}{Fr_1^2} h_1^0 \partial_x b$$
$$+ rc_0 u^0_{1_{|\mathscr{I}}} + \frac{1}{\rho_1}\alpha_0 u^0_{1_{|b}} = 0. \quad (2.30)$$

As we can see, this equation does not contain the viscous effect, so next we derive the second-order approximation. For this aim, we must take into account the terms of order ε ignored before and perform a parabolic correction of the velocity following [14] and [20].

Second-order approximation

First, we define the average of the velocity u_1 as $\bar{u}_1 = \frac{1}{h_1}\int_b^{b+h_1} u_1 \, dz$, and we come back to (2.24), which is written as follows:

$$\partial_{t_1}(h_1 \bar{u}_1) + \partial_x(h_1 \bar{u}_1^2) + \partial_x \int_b^{b+h_1} p_1 dz - p_{1_{|\mathscr{I}}} \partial_x (b + h_1) + p_{1_{|b}} \partial_x b$$
$$- \frac{1}{Re_1}\partial_x \left(\int_b^{b+h_1} \partial_x u_1 dz\right) + \frac{1}{Re_1}(\partial_x w_1 - 3\partial_x u_1 \partial_x (b+h_1))_{|\mathscr{I}}$$
$$- \frac{1}{Re_1}(\partial_x w_1 - 3\partial_x u_1 \partial_x b)_{|b}$$
$$+ \frac{1}{\varepsilon} rc(u_{1_{|\mathscr{I}}} - \varepsilon^2 u_{2_{|\mathscr{I}_\varepsilon}} + \varepsilon^2 w_{1_{|\mathscr{I}}} \partial_x (b+h_1)) + \frac{1}{\rho_1 \varepsilon}\alpha u_{1_{|b}} = 0, \quad (2.31)$$

where we have used $\overline{u_1^2} = \bar{u}_1^2 + \mathscr{O}(\varepsilon^2)$ (see [33]).

From (2.12), we can now write the mass equation for the height $\tilde{h}_1$:

$$\partial_{t_1}\tilde{h}_1 + \partial_x(\tilde{h}_1 \tilde{u}_1) = \mathscr{O}(\varepsilon^2). \quad (2.32)$$

Now, we use the asymptotic hypothesis and previous calculations to simplify (2.31). Using the pressure expression (2.26), we obtain that

$$\partial_x \int_b^{b+h_1} p_1 dz - p_{1_{|\mathscr{I}}} \partial_x (b+h_1) + p_{1_{|b}} \partial_x b$$
$$= \frac{1}{2}\frac{1}{Fr_1^2}\partial_x h_1^2 + \frac{1}{Fr_1^2} h_1 \partial_x b + h_1 \partial_x (p_{1_{|\mathscr{I}}}). \quad (2.33)$$

We use condition (2.18) to write

$$h_1 \partial_x (p_{1_{|\mathscr{I}}}) = 2\varepsilon\mu_{01}\partial_x h_1 \partial_x u_1^0 + \frac{r}{Re_2} h_1 \partial_x (p_{2_{|\mathscr{I}_\varepsilon}}) - 2\varepsilon\mu_{01}\partial_x (h_1 \partial_x u_1^0)$$
$$- h_1 \mu_{01} C_{\mathscr{I}0}^{-1} \partial_x^3 (b+h_1). \quad (2.34)$$

Finally, we insert (2.33) and (2.34) into (2.31) and simplify the terms on the bottom and on the interface $\mathscr{I}(x,t) = b(x) + h_1(x,t)$ using again the divergence-free condition. Thus,

https://doi.org/10.1017/S095679251300020X Published online by Cambridge University Press

we write the second-order approximation of the momentum equation for layer 1:

$$\partial_{t_1}(h_1\bar{u}_1) + \partial_x(h_1\bar{u}_1^2) + \frac{1}{2}\frac{1}{Fr_1^2}\partial_x h_1^2 + \frac{1}{Fr_1^2}h_1\partial_x b - 4\varepsilon\mu_{01}\partial_x(h_1\partial_x\bar{u}_1) + \frac{r}{Re_2}h_1\partial_x(p_{2|_{\mathcal{I}_\varepsilon}}) - h_1\mu_{01}C_{\mathcal{I}0}^{-1}\partial_x^3(b+h_1) + rc_0u_{1|_{\mathcal{I}}} + \frac{1}{\rho_1}\alpha_0 u_{1|_b} = 0. \tag{2.35}$$

To calculate $u_{1|_b}$, we make the parabolic correction of the velocity following [14]. So we come back to (2.10) and look again at the momentum equation to write

$$\mu_{01}\frac{1}{\varepsilon}\partial_z^2 u_1 = \partial_{t_1}u_1^0 + u_1^0\partial_x u_1^0 + \partial_x p_1^0 = \frac{1}{h_1}\left(rc_0u^0_{1|_{\mathcal{I}}} - \frac{1}{\rho_1}\alpha_0 u^0_{1|_b}\right) + \mathcal{O}(\varepsilon),$$

where we have used (2.30) and the divergence-free equation. We use $u_1 = u_1^0 + \mathcal{O}(\varepsilon)$ and integrate this equation to obtain

$$\mu_{01}\frac{1}{\varepsilon}\partial_z u_1 = \frac{1}{h_1}\left(rc_0u_{1|_{\mathcal{I}}} - \frac{1}{\rho_1}\alpha_0 u_{1|_b}\right)(z-b) + \mu_{01}\frac{1}{\varepsilon}\partial_z u_{1|_b} + \mathcal{O}(\varepsilon).$$

Next, by using the bottom friction condition (2.22) and integrating again, we obtain an expression of $\tilde{u}_1$ up to second order:

$$\tilde{u}_1 = u_{1|_b}\left(1 + \varepsilon\frac{\alpha_0}{\rho_1\mu_{01}}(z-b)\left(1 - \frac{z-b}{2h_1}\right)\right) + \varepsilon\frac{rc_0u_{1|_{\mathcal{I}}}}{2\mu_{01}h_1}(z-b)^2 + \mathcal{O}(\varepsilon^2).$$

Thus, its average is

$$\bar{u}_1 = u_{1|_b}\left(1 + \varepsilon\frac{\alpha_0}{\rho_1\mu_{01}}\frac{h_1}{3}\right) + \varepsilon\frac{rc_0h_1}{6\mu_{01}}u_{1|_{\mathcal{I}}} + \mathcal{O}(\varepsilon^2).$$

Finally, we get the value of the velocity at the bottom:

$$u_{1|_b} = \gamma(h_1)\bar{u}_1 - \frac{\varepsilon rc_0}{6\mu_{01}}\gamma(h_1)h_1u_{1|_{\mathcal{I}}} \tag{2.36}$$

with

$$\gamma(h_1) = \left(1 + \frac{\varepsilon\alpha_0}{3\rho_1\mu_{01}}h_1\right)^{-1}.$$

To complete (2.35), it remains to find $\partial_x(p_{2|_{\mathcal{I}_\varepsilon}})$ and $u_{1|_{\mathcal{I}}}$, which depend on layer 2. They will be calculated in the next section, where we develop the study of the second layer.

2.3 Layer 2: thin film flow

As for the first layer, we look for a second-order approximation, so we develop each unknown at first order. We define

$$\tilde{h}_2 = h_2^0 + \varepsilon h_2^1, \quad \tilde{u}_2 = u_2^0 + \varepsilon u_2^1, \quad \tilde{p}_2 = p_2^0 + \varepsilon p_2^1.$$

The *asymptotic regime* for layer 2 affects the viscosity and capillary constants. When surface tension effects are strong, it is essential to have them at the leading order [21], so we assume

$$\nu_2 = \mathcal{O}(\varepsilon), \quad \delta = \mathcal{O}(\varepsilon^{-2}). \tag{2.37}$$

Thus, we have that $Re_2 = \frac{\varepsilon UH}{\nu_2} = \mathcal{O}(1)$ and $C^{-1} = \frac{\delta}{\varepsilon^2 U \rho_2 \nu_2} = \mathcal{O}(\varepsilon^{-5})$ and for simplicity we write $C^{-1} = \varepsilon^{-5} C_0^{-1}$.

Now, we study the velocity equations in (2.13), which can be written as follows:

$$-\partial^2_{z_2} \tilde{u}_2 + \partial_x \tilde{p}_2 = \mathcal{O}(\varepsilon^4), \tag{2.38}$$

$$\partial_{z_2} \tilde{p}_2 = -\varepsilon^4 \frac{Re_2}{Fr_2^2} + \mathcal{O}(\varepsilon^4). \tag{2.39}$$

From the definition of Re_2 and Fr_2, we have $\varepsilon^4 \frac{Re_2}{Fr_2^2} = \varepsilon^2 \frac{gH^2}{U\nu_2} = \mathcal{O}(\varepsilon)$, since $\nu_2 = \mathcal{O}(\varepsilon)$. Thus, we define $\beta_0 = \varepsilon^3 (Re_2/Fr_2^2)$. β_0 is of order 1, so the equation for the pressure reads

$$\partial_{z_2} \tilde{p}_2 = -\varepsilon \beta_0 + \mathcal{O}(\varepsilon^4). \tag{2.40}$$

The mass equation for the second layer comes from the integration of the divergence-free equation. It is necessary to know the velocity u_2 that we calculate from (2.38). In order to establish the integrations limits, recall that for the non-dimensional variables, $z_2 \in [\mathscr{I}_\varepsilon, \eta_\varepsilon]$ (see Section 2.1).

We integrate the incompressibility equation to get

$$\partial_x \int_{\mathscr{I}_\varepsilon}^{\eta_\varepsilon} \tilde{u}_2 \, dz_2 - \tilde{u}_{2\,|_{\eta_\varepsilon}} \partial_x \eta_\varepsilon + \tilde{u}_{2\,|_{\mathscr{I}_\varepsilon}} \partial_x \mathscr{I}_\varepsilon + \tilde{w}_{2\,|_{\eta_\varepsilon}} - \tilde{w}_{2\,|_{\mathscr{I}_\varepsilon}} = 0,$$

that is

$$\partial_x \int_{\mathscr{I}_\varepsilon}^{\eta_\varepsilon} \tilde{u}_2 \, dz_2 - \frac{1}{\varepsilon} \tilde{u}_{2\,|_{\eta_\varepsilon}} \partial_x (b + \tilde{h}_1) - \tilde{u}_{2\,|_{\eta_\varepsilon}} \partial_x \tilde{h}_2 + \frac{1}{\varepsilon} \tilde{u}_{2\,|_{\mathscr{I}_\varepsilon}} \partial_x (b + \tilde{h}_1) + \tilde{w}_{2\,|_{\eta_\varepsilon}} - \tilde{w}_{2\,|_{\mathscr{I}_\varepsilon}} = 0.$$

Taking into account the kinematic conditions on the free surface and on the interface (2.16) and (2.14), we write

$$-\frac{1}{\varepsilon} \tilde{u}_{2\,|_{\eta_\varepsilon}} \partial_x (b + \tilde{h}_1) - \tilde{u}_{2\,|_{\eta_\varepsilon}} \partial_x \tilde{h}_2 + \tilde{w}_{2\,|_{\eta_\varepsilon}} = \frac{1}{\varepsilon^3} \partial_{t_1} (b + \tilde{h}_1) + \partial_{t_2} \tilde{h}_2$$

and

$$\frac{1}{\varepsilon} \tilde{u}_{2\,|_{\mathscr{I}_\varepsilon}} \partial_x (b + \tilde{h}_1) - \tilde{w}_{2\,|_{\mathscr{I}_\varepsilon}} = -\frac{1}{\varepsilon^3} \partial_{t_1} (b + \tilde{h}_1).$$

So, finally the mass equation for the second layer reads

$$\partial_{t_2} \tilde{h}_2 + \partial_x \int_{\mathscr{I}_\varepsilon}^{\eta_\varepsilon} \tilde{u}_2 \, dz_2 = 0. \tag{2.41}$$

We will use (2.38) to obtain an expression for the velocity $\tilde{u}_2$ but first we need to know $\partial_x \tilde{p}_2$ appearing in this equation. We integrate (2.40) from z to η_ε to obtain

$$\tilde{p}_2(z_2) = \tilde{p}_{2\,|_{\eta_\varepsilon}} - \varepsilon \beta_0 (z_2 - \eta_\varepsilon),$$

https://doi.org/10.1017/S095679251300020X Published online by Cambridge University Press

we use the boundary condition at the free surface (2.15b) to write

$$\tilde{p}_{2\,|_{\eta_\varepsilon}} = \varepsilon C_0^{-1} \partial_x^2 \eta_\varepsilon. \tag{2.42}$$

Thus, $\tilde{p}_2(z_2) = \varepsilon C_0^{-1}\partial_x^2\eta_\varepsilon - \varepsilon\beta_0(z_2 - \eta_\varepsilon)$ and

$$\partial_x \tilde{p}_2 = \varepsilon \left(C_0^{-1}\partial_x^3 \eta_\varepsilon + \beta_0 \partial_x \eta_\varepsilon \right) \tag{2.43}$$

does not depend on z_2.

Now, we integrate (2.38) from z to η_ε to find

$$\partial_{z_2}\tilde{u}_2 = \partial_{z_2}\tilde{u}_{2\,|_{\eta_\varepsilon}} + \partial_x \tilde{p}_2 \,(z_2 - \eta_\varepsilon) = \partial_x \tilde{p}_2\,(z_2 - \eta_\varepsilon) + \mathcal{O}(\varepsilon^2),$$

where we have observed that (2.15a) gives $\partial_{z_2}\tilde{u}_{2\,|_{\eta_\varepsilon}} = \mathcal{O}(\varepsilon^2)$.

We integrate again to get $\tilde{u}_2$, now from $\mathcal{I}_\varepsilon$ to z_2, so

$$\tilde{u}_2 = \tilde{u}_{2\,|_{\mathcal{I}_\varepsilon}} + \frac{1}{2}\partial_x \tilde{p}_2 \left((z_2 - \eta_\varepsilon)^2 - \tilde{h}_2^2 \right). \tag{2.44}$$

The value of $\tilde{u}_{2\,|_{\mathcal{I}_\varepsilon}}$ can be found in terms of the pressure $\tilde{p}_2$. In fact, note that from previous equation $\partial_{z_2}\tilde{u}_{2\,|_{\mathcal{I}_\varepsilon}} = -\tilde{h}_2\partial_x\tilde{p}_2$. On the other hand, using the boundary condition at the interface (2.20), we have

$$\partial_{z_2}\tilde{u}_{2\,|_{\mathcal{I}_\varepsilon}} = -c_0 Re_2 \frac{1}{\varepsilon}\left(\tilde{u}_{1\,|_{\mathcal{I}}} - \varepsilon^2 \tilde{u}_{2\,|_{\mathcal{I}_\varepsilon}} \right), \tag{2.45}$$

then

$$\tilde{u}_{2\,|_{\mathcal{I}_\varepsilon}} = \frac{1}{\varepsilon^2}\tilde{u}_{1\,|_{\mathcal{I}}} - \frac{1}{\varepsilon c_0 Re_2}\tilde{h}_2 \partial_x \tilde{p}_2. \tag{2.46}$$

Thus, the velocity $\tilde{u}_2$ is

$$\tilde{u}_2 = \frac{1}{\varepsilon^2}\tilde{u}_{1\,|_{\mathcal{I}}} + \partial_x \tilde{p}_2 \left(-\frac{\tilde{h}_2}{\varepsilon c_0 Re_2} + \frac{1}{2}\left((z_2 - \eta_\varepsilon)^2 - \tilde{h}_2^2 \right) \right). \tag{2.47}$$

Finally, we write the equation for $\tilde{h}_2$ by using (2.41) and (2.47):

$$\partial_{t_2}\tilde{h}_2 + \partial_x\left(\frac{1}{\varepsilon^2}\tilde{h}_2\tilde{u}_1 \right) + \partial_x\left(\tilde{h}_2^2 \left(-\frac{1}{\varepsilon c_0 Re_2} - \frac{1}{3}\tilde{h}_2 \right) \partial_x \tilde{p}_2 \right) = 0, \tag{2.48}$$

where the pressure term is given by (2.43).

Completion of the equation for layer 1

Recall that in (2.35) we must replace the values of $\partial_x(p_{2\,|_{\mathcal{I}_\varepsilon}})$ and $u_{1\,|_{\mathcal{I}}}$. We find the value of the velocity at the interface by using the boundary conditions; from (2.46) we write

$$u_{1\,|_{\mathcal{I}}} = \frac{\varepsilon h_2}{c_0 Re_2}\partial_x p_2 + \mathcal{O}(\varepsilon^2), \tag{2.49}$$

but taking into account (2.43), we can write that

$$u_{1|_{\mathscr{I}}} = \frac{\varepsilon h_2}{c_0 Re_2}\Big(C_0^{-1}\partial_x^3(b+h_1) + \beta_0\partial_x(b+h_1)\Big) + \mathcal{O}(\varepsilon^2). \tag{2.50}$$

Then, we get from (2.36)

$$u_{1|_b} = \gamma(h_1)\bar{u}_1 + \mathcal{O}(\varepsilon^2) \quad \text{with} \quad \gamma(h_1) = \left(1 + \frac{\varepsilon\alpha_0}{3\rho_1\mu_{01}}h_1\right)^{-1} \tag{2.51}$$

and the final equation for layer 1 reads

$$\begin{aligned}
&\partial_{t_1}(h_1\bar{u}_1) + \partial_x(h_1\bar{u}_1^2) + \frac{1}{2}\frac{1}{Fr_1^2}\partial_x h_1^2 + \frac{1}{Fr_1^2}h_1\partial_x b - 4\varepsilon\mu_{01}\partial_x(h_1\partial_x\bar{u}_1)\\
&\quad + \frac{r}{Re_2}h_1\Big(C_0^{-1}\partial_x^3(b+h_1+\varepsilon h_2) + \beta_0\partial_x(\varepsilon h_2)\Big) - h_1\mu_{01}C_{\mathscr{I}0}^{-1}\partial_x^3(b+h_1)\\
&\quad + \frac{r}{Re_2}\varepsilon h_2\Big(C_0^{-1}\partial_x^3(b+h_1) + \beta_0\partial_x(b+h_1)\Big) + \frac{1}{\rho_1}\alpha_0\gamma(h_1)\bar{u}_1 = 0.
\end{aligned} \tag{2.52}$$

3 Final model

In this section, we expose and discuss the final model obtained in the previous section as a formal second-order approximation of the initial problem defined by (2.1)–(2.8). First, we will write this system in dimensional variables and then study the energy balance of the model.

The final deduced model is given in non-dimensional variables by (2.32), (2.43), (2.48) and (2.52). Note that the model contains three equations, mass and momentum for the shallow water flow and the mass equation for the thin film flow.

Next, we present the system in dimensional variables:

$$(\mathrm{M}_1) \equiv \begin{cases}
\partial_t h_1 + \partial_x(h_1 u_1) = 0,\\
\partial_t(h_1u_1) + \partial_x(h_1{u_1}^2) + \frac{1}{2}g\partial_x h_1^2 + gh_1\partial_x b - 4\nu_1\partial_x(h_1\partial_x u_1)\\
\qquad + h_1\Big(\frac{\delta}{\rho_1}\partial_x^3(b+h_1+h_2) + rg\partial_x h_2\Big) - h_1\frac{\delta_{\mathscr{I}}}{\rho_1}\partial_x^3(b+h_1)\\
\qquad + h_2\Big(\frac{\delta}{\rho_1}\partial_x^3(b+h_1) + rg\partial_x(b+h_1)\Big) + \frac{\alpha}{\rho_1}\gamma(h_1)u_1 = 0,\\
\partial_t h_2 + \partial_x(h_2u_1) + \partial_x\left(-{h_2}^2\frac{1}{\rho_2}\Big(\frac{1}{c} + \frac{1}{3\nu_2}h_2\Big)\partial_x p_2\right) = 0,
\end{cases} \tag{3.1}$$

https://doi.org/10.1017/S095679251300020X Published online by Cambridge University Press

with

$$\partial_x p_2 = \delta\, \partial_x^3(b + h_1 + h_2) + \rho_2 g \partial_x(b + h_1 + h_2) \quad \text{and} \quad \gamma(h_1) = \left(1 + \frac{\alpha}{3\nu_1} h_1\right)^{-1}. \tag{3.2}$$

Remark 3.1 The continuity of the tangential stress is usually considered for the interface separating two immiscible viscous fluids and it may correspond to the most realistic case for fluid–fluid interfaces. In our case – due to the different properties of the fluids involved in our system – we found it more appropriate to impose a Navier-slip condition. This condition incorporates the possibility of fluid slip at the interface with the thin lubrication layer [2, 26, 32]. Nevertheless, we would like to know what is the influence of this change into the model. To introduce this condition into the model, we must replace the friction condition (2.6) by the following one:

$$(\sigma_1 \cdot n_{\mathscr{I}})_\tau = -(\sigma_2 \cdot n_{\mathscr{I}})_\tau, \tag{3.3}$$

where by $n_{\mathscr{I}}$ we denote the unitary normal vector to the interface pointing from layer 1 to layer 2. However, we also need an additional condition. When the continuity of the tangential stress is considered, the continuity of velocities at the interface is also usually imposed [17, 29, 31],

$$u_1 = u_2 \quad \text{at } z = \mathscr{I}(x,t). \tag{3.4}$$

By imposing this condition, we obtain the model (M_1) without the term $\partial_x(-h_2^2 \frac{1}{\rho_2}\frac{1}{c}\partial_x p_2)$ in the third equation of (3.1). Note that formally it corresponds to impose an infinity friction coefficient, which implies the continuity of the velocity at the interface.

3.1 Energy of the model

In this subsection, we prove that the model (M_1) admits a dissipative energy inequality up to a second-order term. Then, we propose a variation of this model, called (M_2). The objective is to obtain a model provided with an exact energy balance, as we expose later in Proposition 3.1. The idea of the modification is to change the value of the velocity of layer 1 at the interface written in terms of the pressure p_2.

In order to complete the equation for layer 1, the last step on the derivation has been to replace in the integrated momentum equation the values of $u_{1|_{\mathscr{I}}}$ and $u_{1|_b}$, according to (2.50) and (2.51). As a variation of the model, we propose to change the value of $u_{1|_{\mathscr{I}}}$ to also consider the terms of order ε^2 coming from $\partial_x p_2$. Thus, from (2.43) we write

$$\partial_x p_2 = C_0^{-1}\partial_x^3(b + h_1 + \varepsilon h_2) + \beta_0 \partial_x(b + h_1 + \varepsilon h_2).$$

Then, from (2.49) we deduce the value for the velocity $u_{1|_{\mathscr{I}}}$:

$$u_{1|_{\mathscr{I}}} = \frac{\varepsilon h_2}{c_0 Re_2}\Big(C_0^{-1}\partial_x^3(b + h_1 + \varepsilon h_2) + \beta_0 \partial_x(b + h_1 + \varepsilon h_2)\Big).$$

https://doi.org/10.1017/S095679251300020X Published online by Cambridge University Press

The final system obtained in this case reads as follows:

$$(\mathrm{M}_2) \equiv \begin{cases} \partial_t h_1 + \partial_x(h_1 u_1) = 0, \\ \partial_t(h_1 u_1) + \partial_x(h_1 {u_1}^2) + \dfrac{1}{2} g \partial_x h_1^2 + g h_1 \partial_x b - 4\nu_1 \partial_x(h_1 \partial_x u_1) \\ \quad + h_1 \Big(\dfrac{\delta}{\rho_1} \partial_x^3 (b + h_1 + h_2) + r g \partial_x h_2 \Big) - h_1 \dfrac{\delta_{\mathscr{I}}}{\rho_1} \partial_x^3 (b + h_1) \\ \quad + h_2 \Big(\dfrac{\delta}{\rho_1} \partial_x^3 (b + h_1 + h_2) + r g \partial_x (b + h_1 + h_2) \Big) + \dfrac{\alpha}{\rho_1} \gamma(h_1) u_1 = 0, \\ \partial_t h_2 + \partial_x (h_2 u_1) + \partial_x \left(-{h_2}^2 \dfrac{1}{\rho_2} \Big(\dfrac{1}{c} + \dfrac{1}{3\nu_2} h_2 \Big) \partial_x p_2 \right) = 0, \end{cases} \tag{3.5}$$

with

$$\partial_x p_2 = \delta\, \partial_x^3 (b + h_1 + h_2) + \rho_2 g \partial_x (b + h_1 + h_2) \quad \text{and} \quad \gamma(h_1) = \left(1 + \frac{\alpha}{3\nu_1} h_1 \right)^{-1}. \tag{3.6}$$

We have the following result:

Proposition 3.1 *The models* (M_1) *and* (M_2) *defined by (3.1) and (3.5), respectively, admit an entropy inequality:*

$$\begin{aligned} &\partial_t \left(\frac{u_1^2}{2} + g h_1 (b + \frac{h_1}{2}) + r g h_2 \Big(b + h_1 + \frac{h_2}{2} \Big) \right) \\ &\quad - \frac{\delta}{\rho_1}\, \partial_t \left((h_1 + h_2) \partial_x^2 (b + h_1 + h_2) + \frac{1}{2} (\partial_x (h_1 + h_2))^2 \right) \\ &\quad + \frac{\delta_{\mathscr{I}}}{\rho_1}\, \partial_t \left(h_1 \partial_x^2 (b + h_1) + \frac{1}{2} (\partial_x h_1)^2 \right) \\ &\quad + \partial_x \left(h_1 u_1 \Big(\frac{u_1^2}{2} + g (h_1 + b) \Big) + r g h_2 u_1 (b + 2h_1 + h_2) \right) \\ &\quad - \partial_x \Bigg(4\nu_1 h_1 \partial_x \Big(\frac{u_1^2}{2} \Big) + h_2^2 \frac{1}{\rho_2} \Big(\frac{1}{c} + \frac{1}{3\nu_2} h_2 \Big) \partial_x \Big(\frac{1}{2} (\delta \partial_x^2 (b + h_1 + h_2) \\ &\quad + \rho_2 g (b + h_1 + h_2))^2 \Big) \Bigg) \\ &\quad - \frac{\delta}{\rho_1}\, \partial_x \Big((h_1 + h_2) u_1 \partial_x^2 (b + h_1 + h_2) - (h_1 + h_2) \partial_t (\partial_x (h_1 + h_2)) \Big) \\ &\quad + \frac{\delta_{\mathscr{I}}}{\rho_1}\, \partial_x \Big(h_1 u_1 \partial_x^2 (b + h_1) - h_1 \partial_t (\partial_x h_1) \Big) \\ &\leqslant R. \end{aligned} \tag{3.7}$$

For model (M_2)*, we have an exact dissipative entropy inequality, with*

$$R = R_2 = -4\nu_1 h_1 (\partial_x u_1)^2 - r g^2 h_2^2 \Big(\frac{1}{c} + \frac{1}{3\nu_2} h_2 \Big) \Big(\partial_x (b + h_1 + h_2) \Big)^2 - \frac{\alpha}{\rho_1} \gamma(h_1) u_1^2.$$

For model (M_1), *we have an approximated dissipative entropy inequality, with*

$$R = R_2 + rgu_1\partial_x\left(h_2^2\right) + \frac{\delta}{\rho_1}u_1h_2\partial_x^3\left(h_2\right).$$

Proof. First, we multiply the momentum equation by u_1 and use the mass conservation equation of the first layer for simplification. Then, we obtain

$$\begin{aligned}
&\partial_t\left(\frac{u_1^2}{2} + gh_1\left(b + \frac{h_1}{2}\right)\right) + \partial_x\left(h_1u_1\left(\frac{u_1^2}{2} + g(h_1 + b)\right)\right) - \partial_x\left(4\nu_1h_1\partial_x\left(\frac{u_1^2}{2}\right)\right)\\
&+ \frac{\delta}{\rho_1}h_1u_1\partial_x^3(b + h_1 + h_2) - \frac{\delta_{\mathscr{I}}}{\rho_1}h_1u_1\partial_x^3(b + h_1) + \frac{\delta}{\rho_1}h_2u_1\partial_x^3(b + h_1 + \xi h_2)\\
&+ \frac{\delta}{\rho_1}\partial_th_2\partial_x^2(b + h_1 + h_2) + \frac{\delta}{\rho_1}\partial_x(h_2u_1)\partial_x^2(b + h_1 + h_2)\\
&+ rgh_1u_1\partial_x(h_2) + rgh_2u_1\partial_x(b + h_1 + \xi\, h_2) = -4\nu_1h_1(\partial_xu_1)^2 - \frac{\alpha}{\rho_1}\gamma(h_1)u_1^2, \qquad (3.8)
\end{aligned}$$

where the coefficient $\xi = 0$ for model (M_1) and $\xi = 1$ for model (M_2).

Second, we multiply the equation for the thin film flow by $\delta\partial_x^2(b+h_1+h_2)+\rho_2g(b+h_1+h_2)$ to obtain

$$\begin{aligned}
&\partial_t\left(rg\left(b + \frac{h_2}{2}\right)\right) + rgh_1\partial_th_2 + rg(b + h_1 + h_2)\partial_x(h_2u_1)\\
&\quad + \delta\,\partial_th_2\,\partial_x^2(b + h_1 + h_2) + \delta\,\partial_x(h_2u_1)\partial_x^2(b + h_1 + h_2)\\
&\quad - \partial_x\left(h_2^2\frac{1}{\rho_2}\left(\frac{1}{c} + \frac{1}{3\nu_2}h_2\right)\partial_x\left(\frac{1}{2}(\delta\partial_x^2(b + h_1 + h_2) + \rho_2g(b + h_1 + h_2))^2\right)\right)\\
&= -h_2^2\frac{1}{\rho_2}\left(\frac{1}{c} + \frac{1}{3\nu_2}h_2\right)\left(\delta\partial_x^3(b + h_1 + h_2) + \rho_2g\partial_x(b + h_1 + h_2)\right)^2. \qquad (3.9)
\end{aligned}$$

We use the mass conservation equation to write

$$u_1h_1\partial_xh_2 + h_1\partial_th_2 = \partial_x(rgu_1h_1h_2) - \partial_x(h_1u_1)h_2 + h_1\partial_th_2 = \partial_x(rgu_1h_1h_2) + \partial_t(h_1h_2), \quad (3.10)$$

and to develop the following product affecting the terms with $\delta_{\mathscr{I}}$:

$$\partial_x(h_1u_1)\partial_x^2h_1 = -\partial_t(h_1\partial_x^2h_1) + h_1\partial_t(\partial_x^2h_1) = -\partial_t(h_1\partial_x^2h_1) + \partial_x(h_1\partial_t\partial_xh_1) - \frac{1}{2}\partial_t((\partial_xh_1)^2). \quad (3.11)$$

We make similar calculations for the term with δ.

Finally, by adding (3.8) and (3.9), and taking into account (3.10) and (3.11), we obtain the entropy inequality (3.7).

□

Remark 3.2 For model (M_1), we obtain a dissipative entropy inequality, up to the term

$$rg\,u_1\partial_xh_2^2 + \frac{\delta}{\rho_1}u_1h_2\partial_x^3\left(h_2\right).$$

https://doi.org/10.1017/S095679251300020X Published online by Cambridge University Press

It is of the order of ε^2 because we assumed h_2 to be of the order of ε.

□

4 Numerical tests

We present in this section two academic tests (Sections 4.2 and 4.3). In the first test, a comparison with the numerical results obtained by the viscous bilayer shallow water model proposed in [20] is presented. In the second test, the objective is to show some of the characteristic situations that can be studied with the proposed model. Concretely, we simulate the problem of a pollutant dispersion near the coast. We study the influence of the friction coefficient in order to determine the coastal area affected by the pollutant. As previously, in Subsection 4.1, we present a numerical scheme to discretize the proposed model (3.1)–(3.2).

4.1 Numerical scheme

Before describing the numerical scheme, we observe that the proposed model (3.1)–(3.2) can be written as follows:

$$\partial_t W + \partial_x F(W) = S_1(W)\partial_x b + \partial_x(D(W)\partial_x S_2(W)) + S_{\delta,1}(W) + S_{\delta,2}(W) + S_F(W), \quad (4.1)$$

where if we denote $q_1 = u_1 h_1$, then

$$W = \begin{bmatrix} h_1 \\ q_1 \\ h_2 \end{bmatrix}, \quad F = \begin{bmatrix} q_1 \\ \dfrac{q_1^2}{h_1} + \dfrac{1}{2} g h_1^2 + rgh_1h_2 + \xi\,\dfrac{rg}{2} h_2^2 \\ h_2\dfrac{q_1}{h_1} \end{bmatrix}, \quad S_1(W) = \begin{bmatrix} 0 \\ -g(h_1 + r\,h_2) \\ 0 \end{bmatrix},$$

$$D(W) = \begin{bmatrix} 0 & 0 & 0 \\ 0 & 4\nu_1 h_1 & 0 \\ 0 & 0 & gh_2^2\left(\dfrac{1}{c} + \dfrac{h_2}{3\nu_2}\right) \end{bmatrix}, \quad S_2(W) = \begin{bmatrix} 0 \\ \dfrac{q_1}{h_1} \\ b + h_1 + h_2 \end{bmatrix},$$

$$S_{\delta,1}(W) = \begin{bmatrix} 0 \\ -\bar{\delta}\,r\Big((h_1+h_2)\partial_x^3(b+h_1) + (h_1 + \xi\,h_2)\partial_x^3(h_2)\Big) + \bar{\delta}_{\mathscr{I}} h_1 \partial_x^3(b+h_1) \\ 0 \end{bmatrix},$$

$$S_{\delta,2}(W) = \begin{bmatrix} 0 \\ 0 \\ \bar{\delta}\partial_x\left(h_2^2\left(\dfrac{1}{c} + \dfrac{h_2}{3\nu_2}\right)\partial_x^3(b + h_1 + h_2)\right) \end{bmatrix}, \quad S_F(W) = \begin{bmatrix} 0 \\ -\gamma_1(h_1)\dfrac{q_1}{h_1} \\ 0 \end{bmatrix},$$

https://doi.org/10.1017/S095679251300020X Published online by Cambridge University Press

and

$$\gamma_1(h_1) = \frac{3\,\bar{\alpha}\,v_1}{3v_1 + \bar{\alpha}h_1}, \quad \bar{\alpha} = \frac{\alpha}{\rho_1}, \quad \bar{\delta} = \frac{\delta}{\rho_2}, \quad \bar{\delta}_{\mathscr{I}} = \frac{\delta_{\mathscr{I}}}{\rho_1}.$$

Here, the coefficient $\xi = 0$ corresponds to model (M_1) and $\xi = 1$ to model (M_2).

The Jacobian matrix of $F(W)$ is

$$\mathscr{A}(W) = \begin{bmatrix} 0 & 1 & 0 \\ -u_1^2 + g(h_1 + rh_2) & 2u_1 & gr(h_1 + \xi h_2) \\ -u_1\dfrac{h_2}{h_1} & \dfrac{h_2}{h_1} & u_1 \end{bmatrix}. \tag{4.2}$$

Note that when $h_1 = 0$, we set $u_1 = q_1/h_1 = 0$. Then, the third component of the flux, $(h_2\,q_1/h_1)$, is zero and consequently their derivatives are also zero. That is, in the case that $h_1 = 0$, the third row of $\mathscr{A}(W)$ is set to zero. The eigenvalues of $\mathscr{A}(W)$ are

$$\lambda_1 = u_1 - \mathscr{C}, \quad \lambda_2 = u_1, \quad \lambda_3 = u_1 + \mathscr{C},$$

with

$$\mathscr{C} = \sqrt{gh_1(1-r) + rgh_1\left(1 + \frac{h_2}{h_1}\right)^2 + rg\frac{h_2^2}{h_1}(\xi - 1)}.$$

Remark 4.1 Let us remark that for the characteristic variables, we have that $h_2 = \varepsilon h_1$. If we denote $\varepsilon = h_2/h_1$, then

$$\mathscr{C} = \sqrt{gh_1(1-r) + rgh_1(1+\varepsilon)^2 + rgh_1\varepsilon^2(\xi - 1)}.$$

Thus, when ε tends to zero, we have that $\mathscr{C}$ tends to $\sqrt{gh_1}$. That is, the eigenvalues coincide with those of the transport matrix for the shallow water equations with a passive scalar transport equation.

□

For the discretization of the system, we use a finite volume method. Computing cells $I_i = [x_{i-1/2}, x_{i+1/2}]$ are considered. For simplicity, we suppose that these cells have constant size Δx. Let us define $x_{i+\frac{1}{2}} = i\Delta x$ and $x_i = (i - 1/2)\Delta x$, the centre of the cell I_i. Let Δt be the time step and define $t^{n+1} = t^n + \Delta t$, being $t^0 = 0$.

W_i^n denotes the approximation of the cell averages of the exact solution provided by the numerical scheme:

$$W_i^n \cong \frac{1}{\Delta x}\int_{x_{i-1/2}}^{x_{i+1/2}} W(x, t^n)\,dx. \tag{4.3}$$

The source term $S(W)\partial_x b(x)$ is discretized following the ideas introduced in [5] and [22]. The discretization of $B(W)\partial_x W$ first requires us to interpret this term as a Borel measure (see [10]), depending on the choice of a family of paths linking two given states. Here, the family of segments are considered as in [22]. We also consider a semi-discretization in time of the friction term between the fluid and the bottom.

Let us suppose that the values W_i^n are known. In order to advance in time, we proceed as follows:

• *First step*. We define $W_i^* = [h_{1,i}^* \; q_{1,i}^* \; h_{2,i}^*]^T$ as

$$W_i^* = W_i^n - \frac{\Delta t}{\Delta x}\left(\mathscr{DF}_{i-1/2}^{n,+} + \mathscr{DF}_{i+1/2}^{n,-}\right), \tag{4.4}$$

where $\mathscr{DF}_{i+1/2}^{n,\pm} = \mathscr{DF}_{i+1/2}^{\pm}(W_i^n, W_{i+1}^n)$ is the generalized Roe flux difference computed using the family of segments:

$$\mathscr{DF}_{i+1/2}^{\pm}(W_i, W_{i+1}) = \frac{1}{2}\Big(F(W_{i+1}) - F(W_i) - S_1(W_{i+1/2})(b_{i+1} - b_i) - S_{\delta,1,i+1/2}\Delta x\Big)$$
$$\pm\left(S_{\delta,2,i+1/2} + \frac{1}{2}|\mathscr{A}_{i+1/2}|\Delta_{\mathscr{I}} W_{|_{i+1/2}} + D(W_{i+1/2})\frac{S_2(W_{i+1}) - S_2(W_i)}{\Delta x}\right), \tag{4.5}$$

where $|\mathscr{A}_{i+1/2}|$ is the absolute value of the Roe matrix $\mathscr{A}_{i+1/2}$,

$$W_{i+1/2} = \frac{W_i + W_{i+1}}{2}, \qquad \Delta_{\mathscr{I}} W_{|_{i+1/2}} = \begin{bmatrix} b_{i+1} + h_{1\,i+1} - b_i - h_{1\,i} \\ q_{1\,i+1} - q_{1\,i} \\ h_{2\,i+1} - h_{2\,i} \end{bmatrix},$$

$$S_{\delta,1,i+1/2} = \begin{bmatrix} 0 \\ -\bar{\delta}\, r\Big((h_{2,i+1/2} + h_{1,i+1/2})\phi_{i+1/2}(b + h_1) + (h_{1,i+1/2} + \xi\, h_{2,i+1/2})\phi_{i+1/2}(h_2)\Big) \\ 0 \end{bmatrix}$$
$$+ \begin{bmatrix} 0 \\ \bar{\delta}_{\mathscr{I}} h_{1,i+1/2}\, \phi_{i+1/2}(b + h_1) \\ 0 \end{bmatrix},$$

$$S_{\delta,2,i+1/2} = \begin{bmatrix} 0 \\ 0 \\ \bar{\delta} h_{2,i+1/2}^2 \left(\dfrac{1}{c} + \dfrac{h_{2,i+1/2}}{3\nu_2}\right)\phi_{i+1/2}(b + h_1 + h_2) \end{bmatrix},$$

and

$$\phi_{i+1/2}(\omega) = \frac{1}{\Delta x^3}(\omega_{i+2} - 3\omega_{i+1} + 3\omega_i - \omega_{i-1}).$$

• *Second step*. Semi-discretization in time of the friction term. We define

$$W_i^{n+1} = [h_{1,i}^* \; q_{1,i}^{n+1} \; h_{2,i}^*]^T,$$

where

$$q_{1,i}^{n+1} = \frac{q_{1,i}^*}{1 + \Delta t \gamma_1(h_1^*)/h_1^n}.$$

The scheme is L^∞-stable, for small values of δ, under the Courant-Friedrich-Levy (CFL) condition

$$\frac{\Delta t}{\Delta x}\max_i\left(\frac{|q_{1\,i}|}{h_{1\,i}} + \sqrt{g h_{1\,i}} + \|D(W_i)\|_{L^\infty}/\Delta x\right) \leqslant 1.$$

https://doi.org/10.1017/S095679251300020X Published online by Cambridge University Press

4.2 Test 1: comparison with a viscous bilayer shallow water model

In this first test, we compare the numerical results of the model proposed in this paper with the two-layer viscous shallow water model proposed in [20]. The objective of this test is to show the difference between the proposed model and the two-layer shallow water equations. To deduce this bilayer shallow water model, two immiscible flows with different physical properties have been considered. It includes viscosity and friction effects on the bottom and at the interface level. It is obtained from an asymptotic analysis of non-dimensional and incompressible Navier–Stokes equations with hydrostatic approximation. In order to obtain the viscous effect into the model, a second-order approximation is also considered. The model proposed in [20] reads as

$$\begin{cases} \partial_t h_1 + \partial_x(h_1 u_1) = 0, \\[2mm] \partial_t(h_1 u_1) + \partial_x(h_1 {u_1}^2) + \dfrac{1}{2} g \partial_x h_1^2 + g h_1 \partial_x b + r g h_1 \partial_x h_2 \\ \quad = -\gamma^{-1}\, c\, r \left(\beta \dfrac{\bar{\alpha} h_1}{6\nu_1} u_1 + (u_1 - u_2) \right) + \bar{\delta}_{\mathscr{I}} h_1 \partial_x^3 (b + h_1) \\ \qquad -\beta \bar{\alpha} \left(u_1 + \gamma^{-1} r \dfrac{\bar{\alpha} h_1}{6\nu_1} (u_1 - u_2) \right) + 4\nu_1 \partial_x (h_1 \partial_x u_1), \\[2mm] \partial_t h_2 + \partial_x(h_2 u_2) = 0, \\[2mm] \partial_t(h_2 u_2) + \partial_x(h_2 {u_2}^2) + \dfrac{1}{2} g \partial_x h_2^2 + g h_2 \partial_x (b + h_1) \\ \quad = \gamma^{-1}\, c \left(\beta \dfrac{\bar{\alpha} h_1}{6\nu_1} u_1 + (u_1 - u_2) \right) + 4\nu_2 \partial_x (h_2 \partial_x u_2) + \bar{\delta} h_2 \partial_x^3 (b + h_1 + h_2), \end{cases} \tag{4.6}$$

where

$$\bar{\alpha} = \frac{\alpha}{\rho_1}, \quad \beta = \left(1 + \frac{\bar{\alpha}}{3\nu_1} h_1 \right)^{-1}, \quad \gamma = 1 + \frac{c}{3} \left(r \frac{h_1}{\nu_1} + \frac{h_2}{\nu_2} \right).$$

Recall that c is the coefficient linked to the friction term between both layers (see equation (2.6)), α defines the friction coefficient between the first layer and the bottom (see equation (2.8)), $\bar{\delta} = \delta/\rho_2$ and $\bar{\delta}_{\mathscr{I}} = \delta_{\mathscr{I}}/\rho_1$, with δ and $\delta_{\mathscr{I}}$ the surface and interfacial tension coefficients, respectively.

In order to make a comparison of the numerical results of both models, we consider a very simple test. The domain is set to $[0, 25]$ and is discretized with 200 points. The final time is $t = 2.5$ s. A flat bottom is considered, $b(x) = 0$, and the initial conditions are (see Figure 2): $q_1(x, 0) = q_2(x, 0) = 0$,

$$h_1(x, 0) = 1, \quad h_2(x, 0) = \begin{cases} 0.04 & \text{if } x \in [12, 13], \\ 0 & \text{otherwise.} \end{cases}$$

No flux boundary conditions are considered, i.e. $\partial_x h_i = 0$, $\partial_x(h_i u_i) = 0$ for $i = 1, 2$. From a numerical point of view, they are imposed by considering a ghost cell where the value of the unknowns coincides with the value at the boundary cell. Let us remark that at the

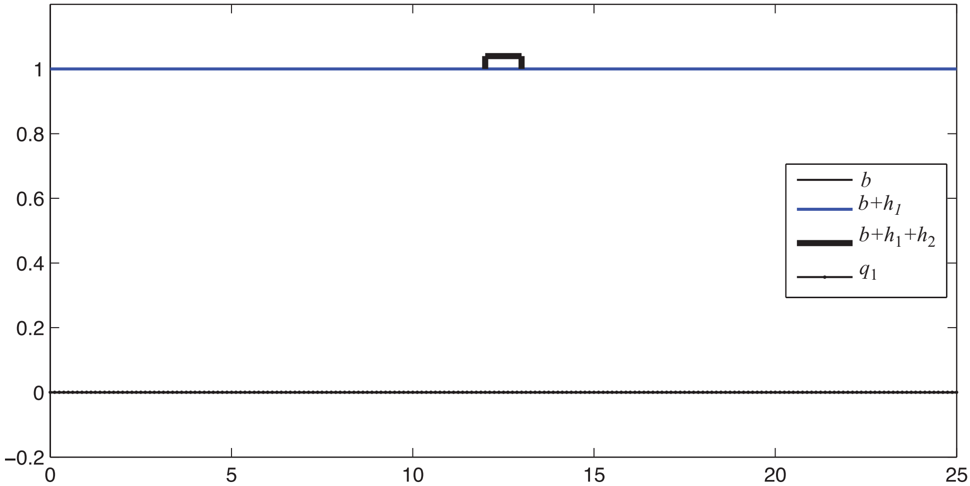

FIGURE 2. (Colour online) Test 1. Initial conditions for test 1 with flat solid surface, a local perturbation in h_2 and null fluxes for both fluids.

contact points between the pollutant drop and the liquid, it is not necessary to use any special numerical treatment since a Navier slip is incorporated in (3.1)–(3.2).

For this test, the friction coefficients are set to $c = 1$ and $\bar{\alpha} = 10^{-3}$. We set $\rho_1 = 1,027$, corresponding to the sea water, and $\rho_2 = 920$, $\delta = 0.033$, corresponding to the density and tension surface coefficient of a marine residual fuel. The interfacial tension coefficient is set to $\delta_{\mathscr{I}} = 0.027$, corresponding to an oil/sea-water interface (see [16]). In the areas where $h_2 = 0$, we set $\delta_{\mathscr{I}} = 0.072$, corresponding to the sea-water surface tension.
Then, we have

$$r = 0.8958, \quad \bar{\delta} = \frac{\delta}{\rho_2} = 0.3587 \times 10^{-4}, \quad \bar{\delta}_{\mathscr{I}} = \frac{\delta_{\mathscr{I}}}{\rho_1} = \begin{cases} 0.2629 \times 10^{-4} & \text{if } h_2 > 0, \\ 0.7010 \times 10^{-4} & \text{if } h_2 = 0. \end{cases} \tag{4.7}$$

The water viscosity and the pollutant viscosity are set to

$$\nu_1 = 10^{-6}, \quad \nu_2 = 5.9783 \times 10^{-4}. \tag{4.8}$$

In Figure 3, the evolution of the layers for the proposed model, coupling Saint Venant and Reynolds lubrication equations (SVR in what follows), is compared with the viscous bilayer shallow water system (2SW in what follows). We can observe that the evolution of the upper layer is completely different for these two models. The layer on the top is supposed to be a thin film flow, so the velocity of this layer must be lower than the velocity of the water fluid considered on the shallow water layer. These hypotheses on the relative velocities and thicknesses of the layers have been taken into account to deduce the SVR model. It corresponds to the behaviour that we observe in this test, where the pollutant drop remains enclosed over the water layer (see Figure 3, left column). In Figure 4, a zoom of the evolution of the free surface near the pollutant is presented. On the contrary, if we look at the 2SW model solutions (Figure 3, right column), we can see

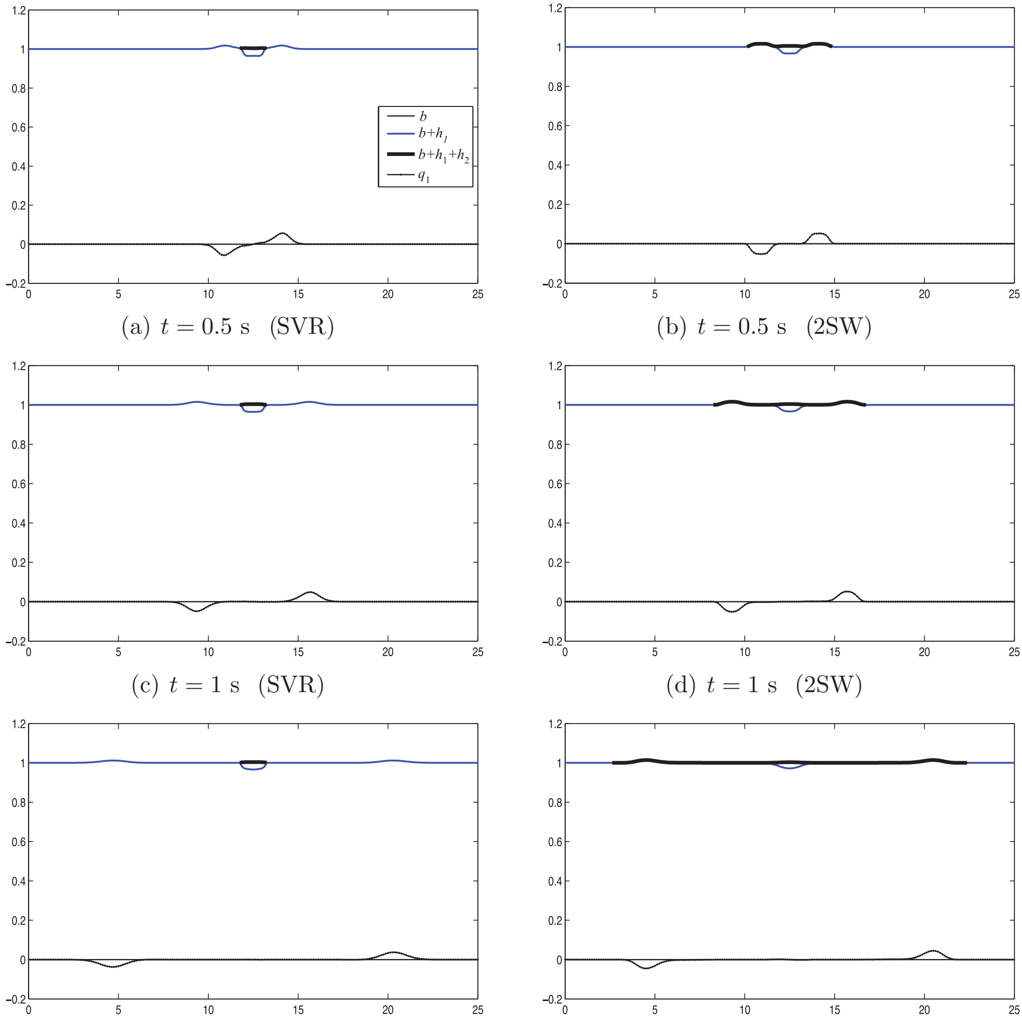

(a) $t = 0.5$ s (SVR) (b) $t = 0.5$ s (2SW)

(c) $t = 1$ s (SVR) (d) $t = 1$ s (2SW)

(e) $t = 2.5$ s (SVR) (f) $t = 2.5$ s (2SW)

FIGURE 3. (Colour online) Test 1. Evolution of water and pollutant layers at time $t \in \{0.5, 1, 2.5\}$ s. Left: proposed model (SVR). Right: viscous bilayer shallow water system (2SW).

that the velocity of the pollutant layer is very similar to the velocity of the water layer, which makes the pollutant to spread all over the water layer. From the physical point of view, this is the situation that one finds when the two fluids have similar thicknesses but not for the case studied here. Let us remark that to derive the 2SW model, the same shallow water assumptions as for both layers, with different density and viscosity, have been considered.

With this numerical test, we point out that the 2SW model is not well adapted to study the evolution of a thin pollutant layer over water. It is necessary to consider a Reynolds lubrication theory to model the evolution of the thin film flow.

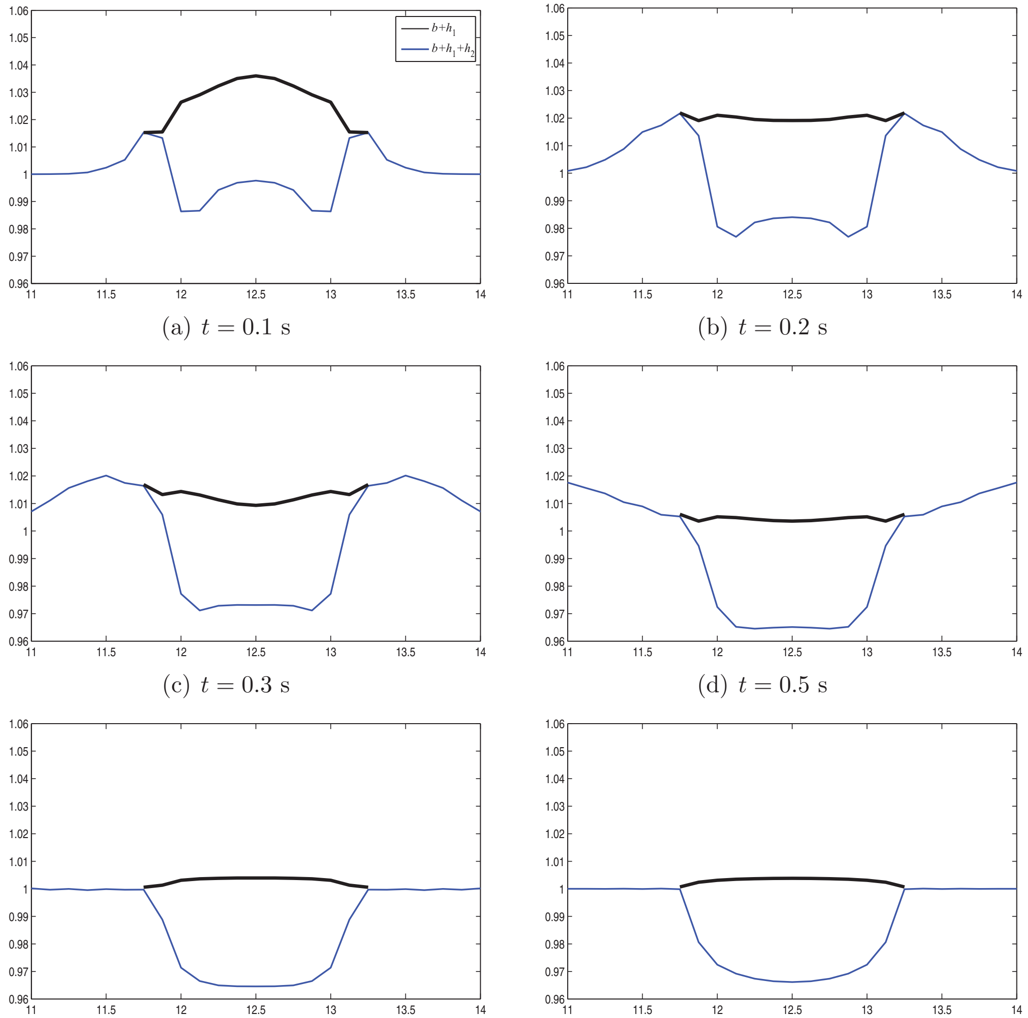

(a) $t = 0.1$ s (b) $t = 0.2$ s (c) $t = 0.3$ s (d) $t = 0.5$ s (e) $t = 1$ s (f) $t = 2.5$ s

FIGURE 4. (Colour online) Test 1. Details of the dynamics of the free surface centred around the pollutant, on the region $11 < x < 14$, for water and pollutant layers for the (SVR) model at time $t \in \{0.1, 0.2, 0.3, 0.5, 1, 2.5\}$ s.

4.3 Test 2: pollutant dispersion near the coast

The aim of this test is to show some of the characteristic situations in which the proposed model can be used. Concretely, we study the dispersion of a pollutant near the coast, for an academic case. The domain is $[0, 12]$ and it is discretized with 200 points. The bottom is defined by the following function:

$$b(x) = \begin{cases} \mathrm{e}^{\frac{-(x-8)^2}{10}} & \text{if } x \leqslant 8, \\ 1 + \mathrm{e}^{\frac{-(x-20)^2}{50}} - e^{\frac{-12^2}{50}} & \text{if } x > 8. \end{cases}$$

https://doi.org/10.1017/S095679251300020X Published online by Cambridge University Press

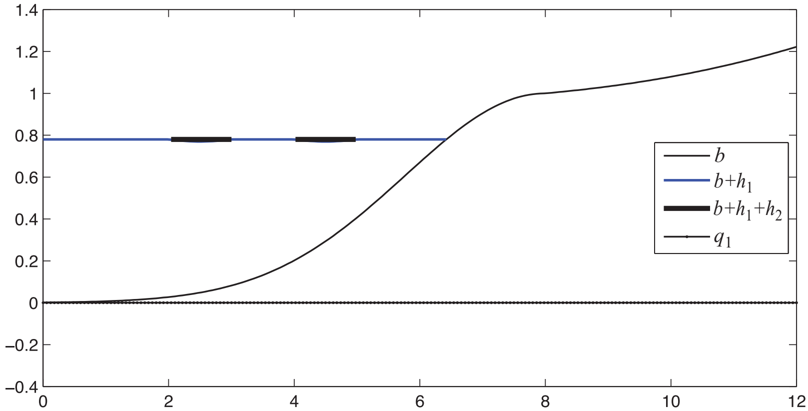

FIGURE 5. (Colour online) Test 2. Initial condition for test 2 with bottom surface simulating a coast profile, two pollutant sticks over water and null fluxes for both fluids.

As an initial condition, we set a horizontal free surface and two pollutant slicks (see Figure 5). Concretely,

$$q_1(x,0) = q_2(x,0) = 0, \quad h_1(x,0) = \max(0.78 - b(x), 0) - h_2(x,0),$$

$$h_2(x,0) = \begin{cases} 10^{-2} \max(\sin(\pi x), 0) & \text{if } x \in [2,5], \\ 0 & \text{otherwise.} \end{cases}$$

As a boundary condition, the velocity on $x = 0$ is imposed:

$$u_1(0,t) = 0.4 \sin\left(\frac{t\,\pi}{5}\right). \tag{4.9}$$

The evolution of the water surface and the pollutant slick is computed for $t \in [0,8]$ s. As in the first test, the values of r, v_1, v_2, $\bar{\delta}$ and $\bar{\delta}_{\mathscr{I}}$ are defined by (4.7) and (4.8). We also set the friction coefficient between the fluid and the bottom as $\bar{\alpha} = 10^{-3}$. In this test, we study the influence of c – the friction coefficient between the pollutant and the water – on the spread of the pollutant over the coast. We consider several values of c in $[10^{-3}, 1]$.

For the numerical simulation, we apply the wet/dry numerical treatment proposed in [3].

In Figure 6, the fluid and pollutant evolution are presented for $t \in \{2,3,4,5,7,8\}$ s with $c = 10^{-1}$. This period includes one period wave of the fluid induced by the boundary condition imposed for u_1 (equation (4.9)).

In Figures 6(a) and (b), we can observe how first the pollutant slicks are transported separately. Note that at these times we are simulating that the tide rises, so the velocity of the water layer is higher at the left of the domain than at the right. Consequently, the first oil slick moves with a higher velocity than the second one. This leads both oil slicks to connect some time later, as we can observe in Figures 6(c) and (d). The maximum imposed velocity at the boundary condition is reached at $t = 2.5$ s. At $t = 5$ s, the imposing velocity turns negative. Then, in Figures 6(e) and (f), we observe that the water comes back, as well as the transport of the oil pollutant, which has been spread near the coastline.

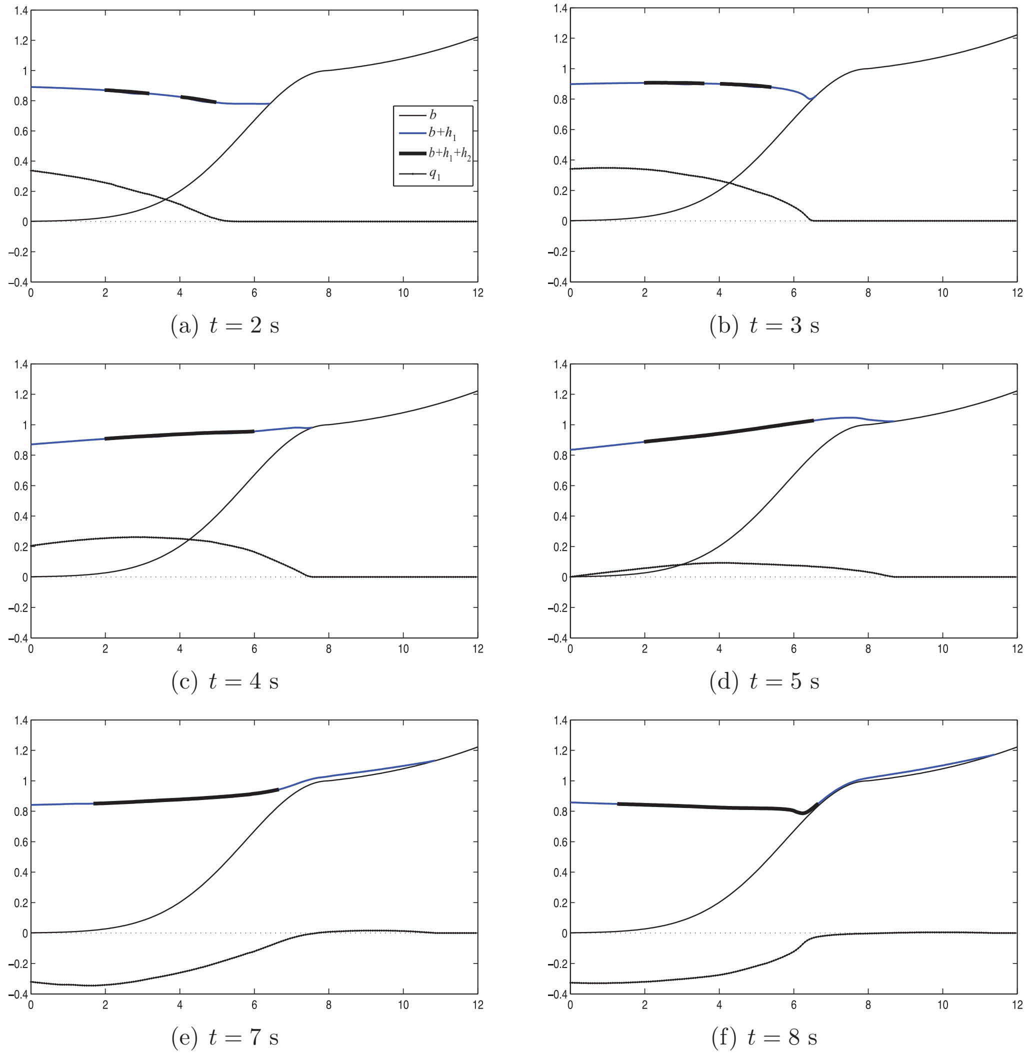

FIGURE 6. (Colour online) Test 2. Evolution of water and pollutant layers at time $t \in \{2, 3, 4, 5, 7, 8\}$ s for the proposed model.

In Figure 7, the simulation at $t = 8$ s for $c \in \{10^{-3}, 10^{-2}, 10^{-1}, 1\}$ is presented. We check the influence of the friction coefficient on the range of the pollutant spread. We can observe that the spread of the pollutant layer is not linearly dependent on the friction coefficient c. Moreover, when the value of c is smaller, the pollutant is nearest to the shoreline.

In order to study the influence of c, we present in Figure 8 the values of $x_{\max}$, the maximum value of x such that $h_2(x,t) > 0$, for $c \in \{j \times 10^{-3}, j \times 10^{-2}, j \times 10^{-1}, 1\}$, with $j = 1, \ldots, 9$. We can observe that when $c \in [0.1, 1]$, $x_{\max}$ is almost constant. When $c \in [10^{-2}, 10^{-1}]$, the value of $x_{\max}$ begins to increase. And for $c \leqslant 10^{-2}$, the value of $x_{\max}$ increases with a large slope. We can conclude that the spread of the pollutant layer,

https://doi.org/10.1017/S095679251300020X Published online by Cambridge University Press

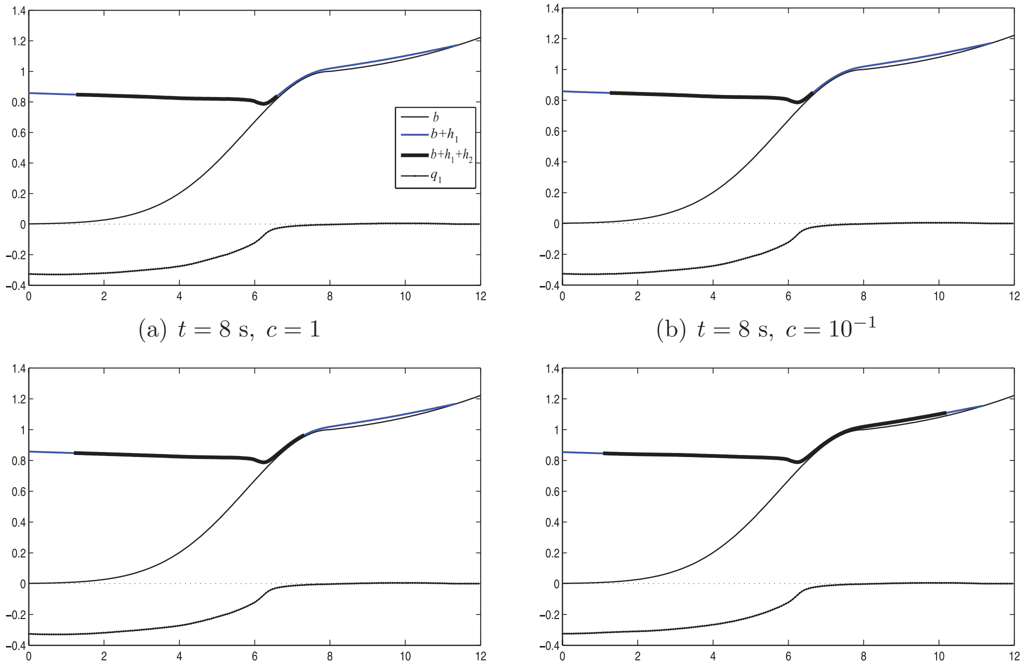

(a) $t = 8$ s, $c = 1$ (b) $t = 8$ s, $c = 10^{-1}$

(c) $t = 8$ s, $c = 10^{-2}$ (d) $t = 8$ s, $c = 10^{-3}$

FIGURE 7. (Colour online) Test 2. Water and pollutant profiles for fixed time $t = 8$ and for several values of the friction coefficient $c \in \{1, 10^{-1}, 10^{-2}, 10^{-3}\}$ for the proposed model.

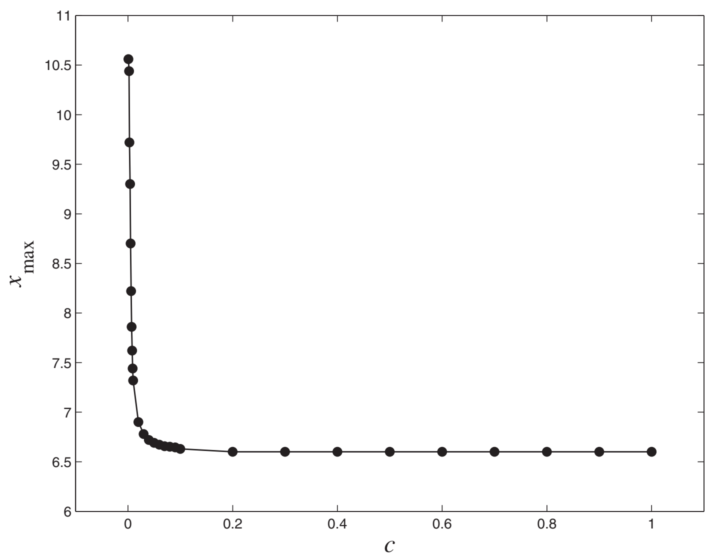

FIGURE 8. Test 2. Maximum value of x such that $h_2(x, t) > 0$ (denoted by $x_{\max}$) in terms of the friction coefficient $c \in \{j \times 10^{-3}, j \times 10^{-2}, j \times 10^{-1}, 1\}$ for $j = 1, \ldots, 9$.

https://doi.org/10.1017/S095679251300020X Published online by Cambridge University Press

as a function of c, can be approximated by a function with a vertical and a horizontal asymptote.

Moreover, since the model has been deduced by supposing that $h_2/h_1 = \mathcal{O}(\epsilon)$ (if $h_1 > 0$), we have checked if this condition is verified in the numerical simulations, with $\epsilon = 10^{-1}$. We obtain that $h_2/h_1 = \mathcal{O}(\epsilon)$ in the zones where $h_1 > 0$ for $c \geqslant 3 \times 10^{-3}$. For $c < 3 \times 10^{-3}$, it is not verified near the shoreline.

Note that even if the numerical simulation for $c = 10^{-3}$ and $c = 2 \times 10^{-3}$ does not verify that $h_2/h_1 = \mathcal{O}(\epsilon)$ in all the points of the domain, we observe in Figure 8 that the values of $x_{\max}$ are reasonable in comparison with the behaviour observed for the values of $x_{\max}$ corresponding to $c \geqslant 3 \times 10^{-3}$.

5 Conclusions

A new bilayer model is presented in this paper to simulate the transport of a viscous thin layer of fluid over water. For this aim, two kinds of equations have been considered for each layer: the Reynolds lubrication equation to model the upper layer and a shallow water model to describe the evolution of the water layer. An analysis of two different scales in space and time is carried out in the derivation of the coupling model. The model can be applied to simulate a transport of a viscous pollutant over water. We have proved that the model verifies, up to a second-order term, a dissipative entropy inequality. Moreover, we have proposed a correction of the model that takes into account the second-order extension for the pressure law. This version of the model verifies an exact dissipative entropy inequality. Finally, some academic numerical tests are presented. The objective of the first test is to show the difference between the proposed model and the bilayer shallow water equations. We have observed that the bilayer shallow water model is not well adapted to study the evolution of a thin pollutant layer over water. It is necessary to consider a Reynolds lubrication theory to model the evolution of the thin film flow, as we consider in the proposed model. In the second test, we simulate the problem of a pollutant dispersion near the coast. In this test, we have studied the influence of the friction coefficient on the amplitude of the coastal area affected by the pollutant.

Acknowledgements

This research has been partially supported by the Spanish Government Research project MTM2009-07719. The authors thank the Instituto Universitario de Investigación de Matemáticas de la Universidad de Sevilla (IMUS) for the grant awarded to J.D.Z.

References

[1] Audusse, E. (2005) A multilayer Saint-Venant model. *Disc. Cont. Dyn. System.* B **5**(2), 189–214.

[2] Blyth, M. G. & Pozrikidis, C. (2005) Stagnation-point flow against a liquid film on a plane wall. *Acta Mech.* **180**, 203–219.

[3] Castro, M. J., Ferreiro, A. M., García, J. A., González, J. M., Macías, J., Parés, C. & Vázquez, M. E. (2005) On the numerical treatment of wet/dry fronts in shallow flows: Applications to one-layer and two-layer systems. *Math. Comp. Model.* **42**(3–4), 419–439.

[4] Castro Díaz, M. J., Fernández-Nieto, E. D. & Ferreiro, A. M. (2008) Sediment transport models in Shallow Water equations and numerical approach by high order finite volume methods. *Comput. Fluids* **37**, 299–316.

[5] Chacón, T., Domínguez, A.& Fernández, E. D. (2004) Asymptotically balanced schemes for non-homogeneous hyperbolic systems – application to the Shallow Water equations. *C. R. Acad. Sci. Paris* I **338**, 85–90.

[6] Chueskov, I. D., Raugel, G. & Rekalo, A. M. (2005) Interface boundary value problem for the Navier–Stokes equations in thin domains. *J. Differ. Equ.* **208**, 449–493.

[7] Cimatti, G. (1987) A rigorous justification of the Reynolds equation. *Q. Appl. Math.* **XLV**(4), 627–644.

[8] Cope, W. F. (1949) The hydrodynamic theory of film lubrication. *Proc. R. Soc. London, Ser. A* **197**, 201–217.

[9] Cordier, S., Lucas, C. & Zabsonré, J. D. D. (2012) A two time-scale model for tidal bed-load transport. *Commun. Math. Sci.* **10**, 875–888.

[10] Dal Maso, G., LeFloch, P. G. & Murat, F. (1995) Definition and weak stability of nonconservative products. *J. Math. Pure Appl.* **74**, 483–548.

[11] Dowson, D. (1962) A generalized Reynolds equation for fluid-film lubrication. *Int. J. Mech. Sci.* **4**, 159–170.

[12] Elrod, H. G. (1960) A derivation of the basic equations for hydrodynamics lubrication with a fluid having constant properties. *Q. Appl. Math.* **27**, 349–385.

[13] Ferrari, S. & Saleri, F. (2004) A new to dimensional shallow-water model including pressure effects and slow varying bottom topography. *M2AN* **38**(2), 211–234.

[14] Gerbeau, F. & Perthame, B. (2001) Derivation of viscous Saint–Venant system for laminar shallow-water: Numerical validation. *Disc. Cont. Dyn. Syst.* B **1**(1), 89–102.

[15] Hulscher, S. (1996) *Formation and Migration of Large-Scale, Rhythmic Sea-Bed Patterns: A Stability Approach*, Ph.D. thesis, Utrecht University.

[16] Konno, A. & Izumiyama, K. (2002) On the relationship of the oil/water interfacial tension and the spread of oil slick under ice cover. In: *Proceedings of the 17th International Symposium on Okhotsk Sea and Sea Ice*, pp. 275–282, Hokkaido, Japan.

[17] Koster, J. N. (1994) Multilayer fluid dynamics of immiscible fluids. In: *Second Microgravity Fluid Physics Conference*, pp. 65–71, Lewis Research Center, NASA.

[18] Marche, F. (2005) *Theoretical and Numerical Study of Shallow Water Models. Applications to Nearshore Hydrodynamics*. Ph. D. Thesis, University of Bordeaux.

[19] Marusic-Paloka, E. & Starcevic, M. (2009) Derivation of Reynolds equation for gas lubrication via asymptotic analysis of the compressible Navier–Stokes system. *Nonlinear Anal.: Real World Appl.* **11**, 4565–4571.

[20] Narbona-Reina, G., Zabsonré, J. D. D., Fernández-Nieto, E. D. & Bresch, D. (2009) Derivation of a bi-layer Shallow-Water model with viscosity. Numerical validation. *Comput. Model. Eng. Sci.* **43**(1), 27–71.

[21] Oron, A., Davis, S. H. & Bankoff, S. G. (1997) Long scale evolution of thin films. *Rev. Mod. Phys.* **69**(3), 931–980.

[22] Parés, C. & Castro, M. J. (2004) On the well-balance property of Roe's method for nonconservative hyperbolic systems. Applications to shallow-water systems. *ESAIM-Math. Model. Num.* **38**(5), 821–852.

[23] Peybernes, M. (2006) *Analyse de problème mathématiques de la mécanique des fluides de type bi-couche et à frontière libre*. Ph.D. thesis, University of Pascal Paoli.

[24] Reynolds, O. (1886) On the theory of lubrication and its application to Mr. Beauchamp Tower's experiment. *Phil. Trans. R. Soc. London* Part I, **52**, 228–310.

[25] Roos, P. C. (2004) *Seabed Pattern Dynamics and Offshore Sand Extraction*, Ph.D. thesis, University of Twente.

[26] Santra, B., Dandapat, B. S. & Andersson, H. I. (2007) Axisymmetric stagnation-point flow over a lubricated surface. *Acta Mech.* **194**(1–4), 1–10.

[27] Schuttelaars, H. (1997) *Evolution and Stability Analysis of Bottom Patterns in Tidal Embayment*, Ph.D. thesis, Utrecht University.

[28] Shukla, J. B., Kumar, S. & Chandra, P. (1980) Generalized Reynolds equation with slip at bearing surfaces: Multiple-layer lubrication theory. *Wear* **60**, 253–268.

[29] Stone, H. A. & Bush, J. W. M. (1996) Time-dependent drop deformation in a rotation high viscosity fluid. *Q. App. Math.* **54**(3), 551–556.

[30] Wannier, G. H. (1950) A Contribution to the hydrodynamics of lubrication. *Q. Appl. Math.* **88**, 1–32.

[31] Wilkes, J. (2006) *Fluid Mechanics for Chemical Engineers with Microfluidics and CFD*. Indiana, IN: Prentice Hall.

[32] Yeckel, A., Strong, L. & Middleman, S. (1994) Viscous film flow in the stagnation region of the jet impinging on planar surface. *AIChE J.* **40**, 1611–1617.

[33] Zabsonré, J. D. D. (2008) *Modèles Visqueux en Sédimentation et Stratification: Obtention Formelle, Stabilité Théorique et Schémas Volumes Finis Bien Équilibrés*. Ph.D. thesis, University of Savoie.

[34] Zabsonré, J. D. D. & Narbona-Reina, G. (2009) Existence of a global weak solution for a 2D viscous bi-layer shallow water model. *Nonlinear Anal.: Real World Appl.* **10**, 2971–2984.